Presented at the COMSOL Conference 2009 Milan

The 2002-2003 eruptive event: a laboratory for testing kinematics of Mt. Etna eastern flank

Dr. Fabio Pulvirenti

Catania University – Geological Science Department

2002 Etna Eruption

Overview

26 October 2002 20:25 (GMT): a seismic swarm takes place 1 km eastwards from central craters and about 1km over the sea level.

27 October 03:10 (GMT): an intense explosive activity with lava effusion and ash columns begins at the south flank from a fracture oriented N-S at 2750 m

During the first hours of 27 October, and until 28 October, a long field of eruptive fissures, parallel to the NE Rift, begin to propagate towards the north-east flank. The opening of these fissures is accompanied and followed by seismic activity.

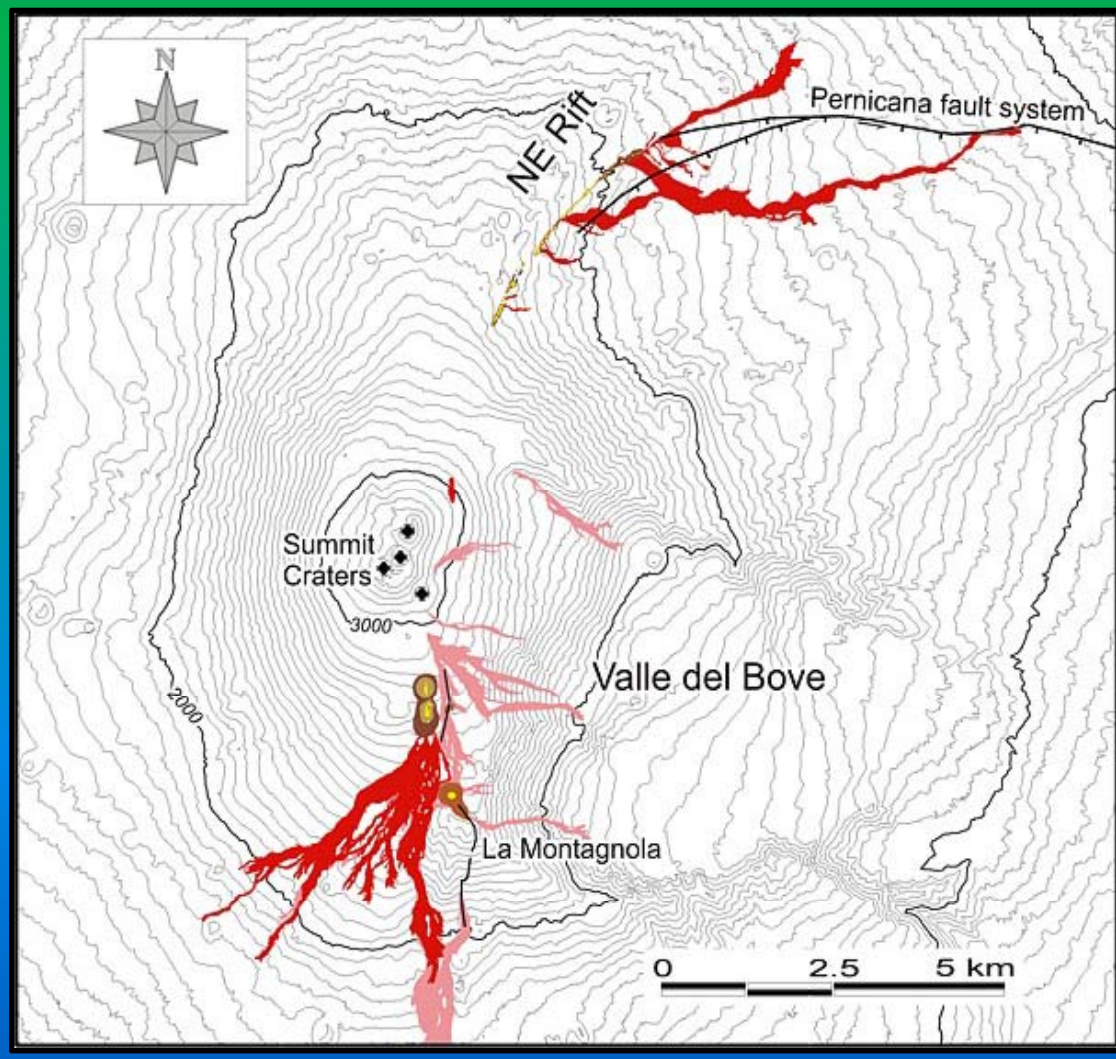

2002 Etna Eruption

Overview

On 27 October (01.28 GMT), seismicity (depth max = 3.5 km b.s.l.; Mmax =3.8) involves the western tip of the WNW-ESE trending Pernicana fault on the north-eastern flank of the volcano. destroying the Piano Provenzana tourist station

29/10/2002 10.02 GMT: Timpe fault system is reactivated with dextral-oblique motion *(*MONACO *et al, 2005) between* San Giovanni Bosco and Santa Venerina (earthquake of M=4.4)

29/10/2002; (16.39 GMT)an earthquake of M=4 takes places in Guardia village.

The eruption on the north side lasted 9 days with emission of lava fluxes and an intense Strombolian activity. On the south side it continued until January 28, 2003.

The analytical inversion model

Inversion procedures of ground data based on Okada analytical model indicated that displacements observed can be interpreted as the response of the volcanic edifice to a double dike intrusion: a fast uprise of an eccentric dike at south flank that triggered the eruption and a lateral intrusion of a second dike at north-east flank that was the principal cause of the deformation observed.

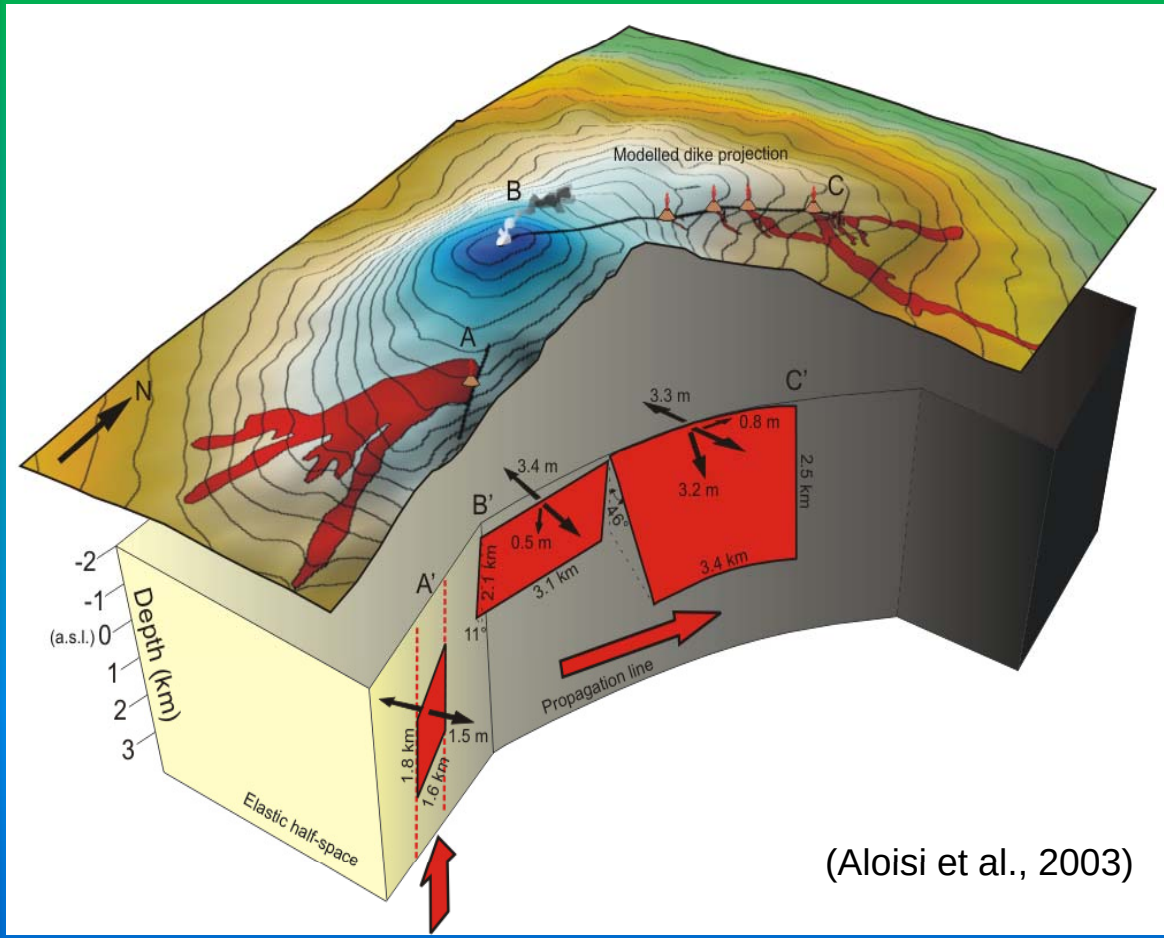

(Aloisi et al., 2003)

2002 Eruption as seen with FEM

Overview

The aim of our work is to reproduce the 2002-2003 Etna eruptive event and to compare the surface displacements calculated numerically with that recorded by GPS stations and already modelled by analytical methods. A parametric model in an elastic regime is performed.

The model planning is organized in the following phases:

- Geometry creation: The Computational domain and all the internal structures are designed;
- Subdomain settings: All subdomains are set by physics characteristics and gravitational load can be applied ;
- Boundary settings: Application of all the constrain conditions for internal or perimetric surfaces of the computational domain;
- Mesh generation: Mesh parameters are set;
- Solving: All the solving settings (solver type, numer of iteration etc.)

2002 Eruption as seen with FEM

Geometry creation

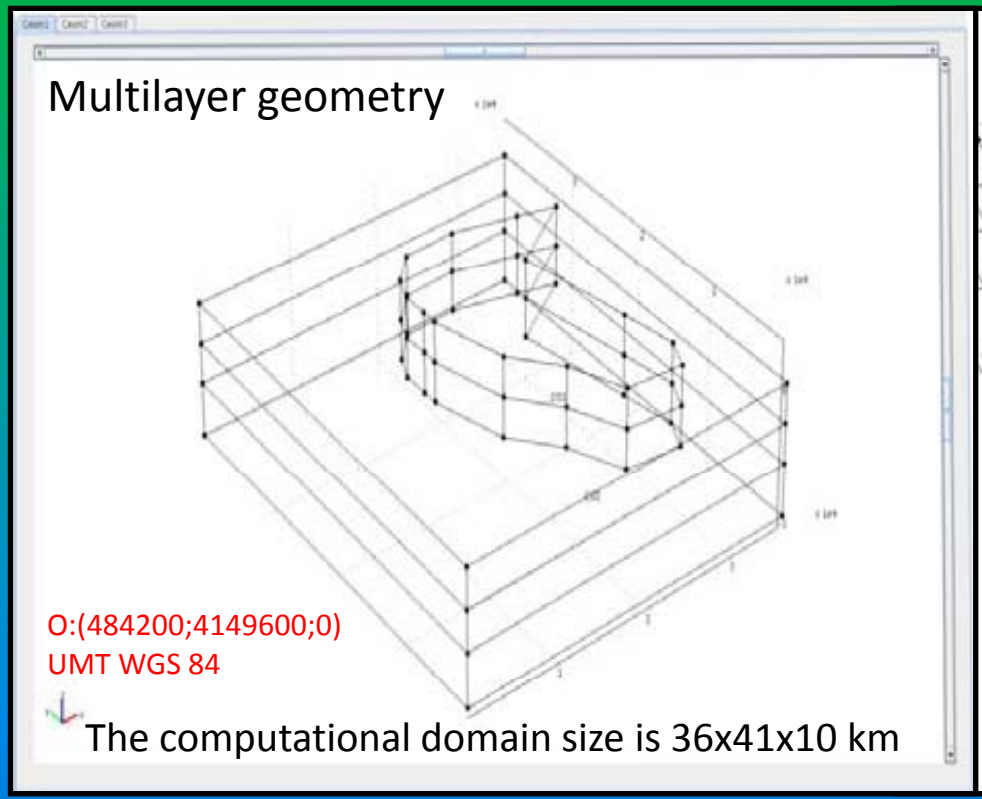

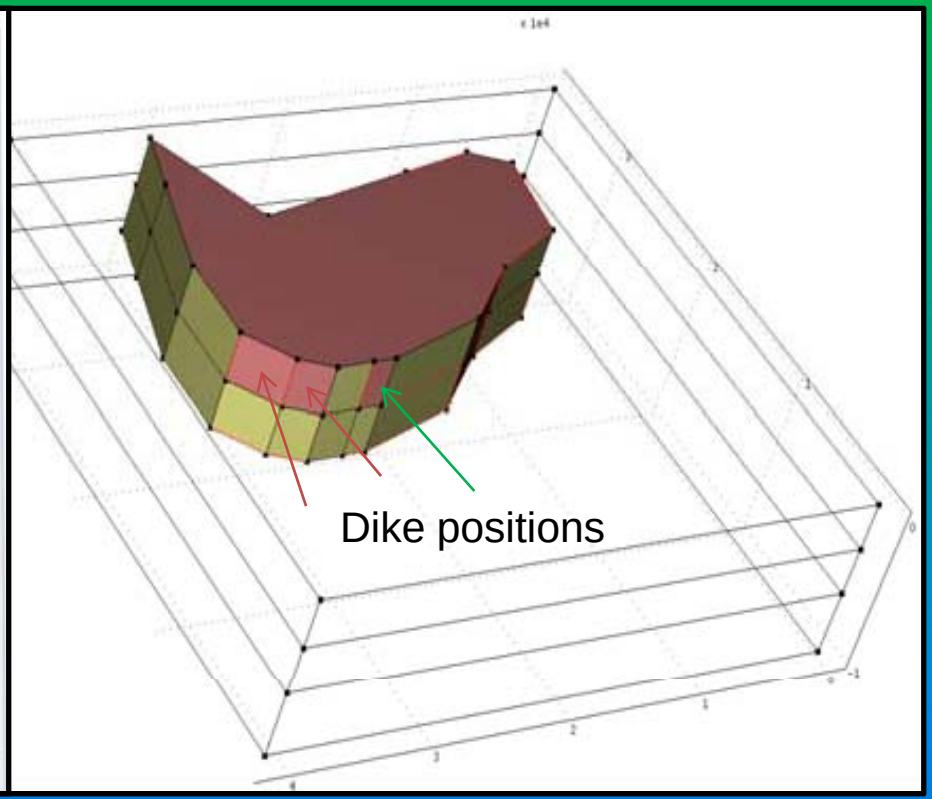

The original domain is divided in 3 layers:
1) From sea level to -3km
2) From -3km to -6km
3) From -6km to -10 km

Using the work plane a structure is extruded and integrated into the domain. Some perimetric boundaries correspond to the position of the faults, others to the position of the dikes.

2002 Eruption as seen with FEM

Geometry creation

Our model is formed by the volcano edifice, a clay substratum and a layer with Hyblean succession and crystalline basement.

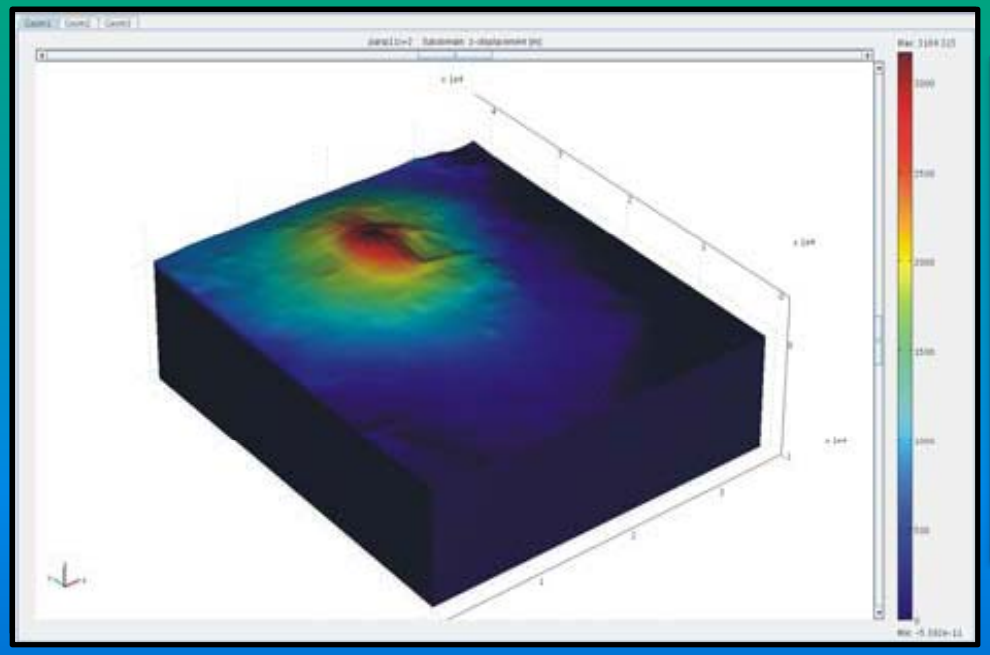

Volcano surface is generated from the top of the first layer (sea level) by importing a DEM file with 1000 m resolution. DEM is read and reproduced by the *moving mesh* procedure.

2002 Eruption as seen with FEM

Geometry creation

Geological profiles (Monaco et al.,2008) show the existence of a sedimentary substratum (clay) beneath the volcano; its upper surface has a nearly convex profile reaching an height of 1250 m under the central craters zone and minor heights elsewhere, with some superficial outcrops. It reaches a -1km depth.

Choosing some points for which the height of the clay is noted, an interpolation surface can be generated. We called the function for this surface *argilla(x,y).*

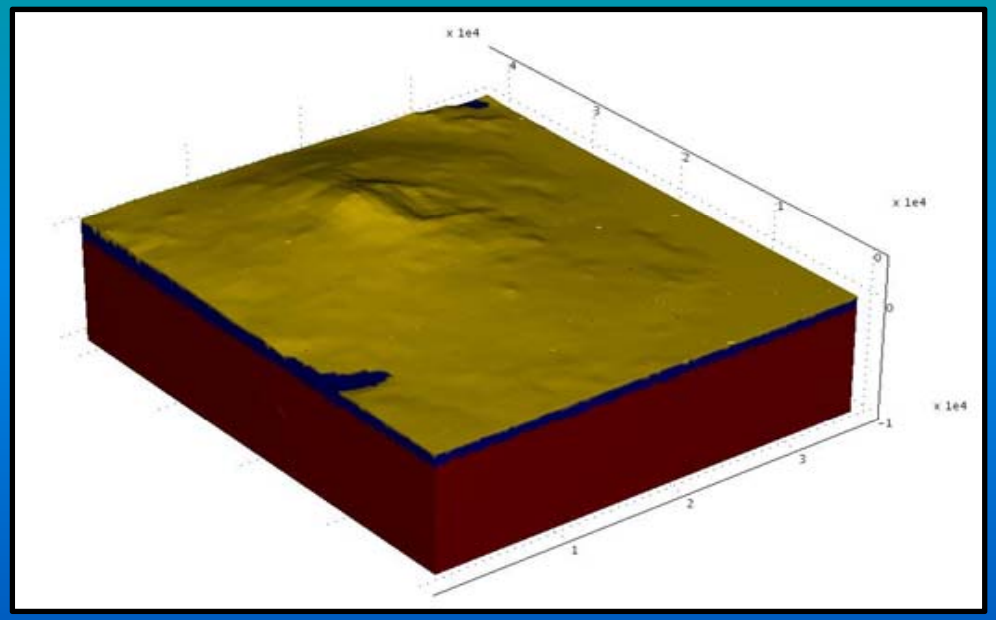

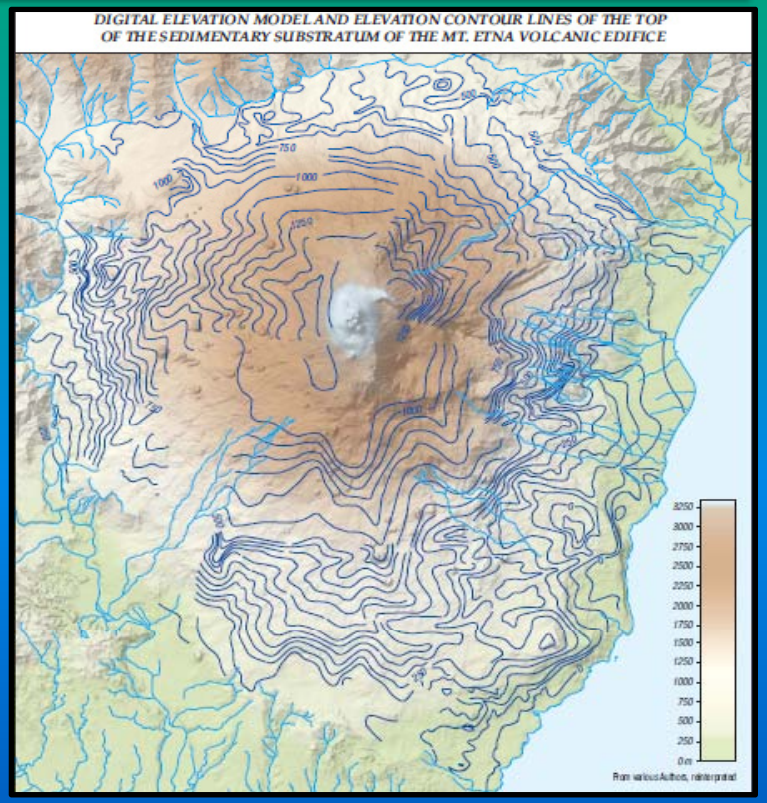

2002 Eruption as seen with FEM

Subdomain settings

Subdomains settings allow to set all the physical conditions of the different layers.

(z>=argilla(x,y))*(30e9[Pa])+(z>=-1000&&z<argilla(x,y))*(10e9[Pa])+(z<-1000)*(40e9[Pa])

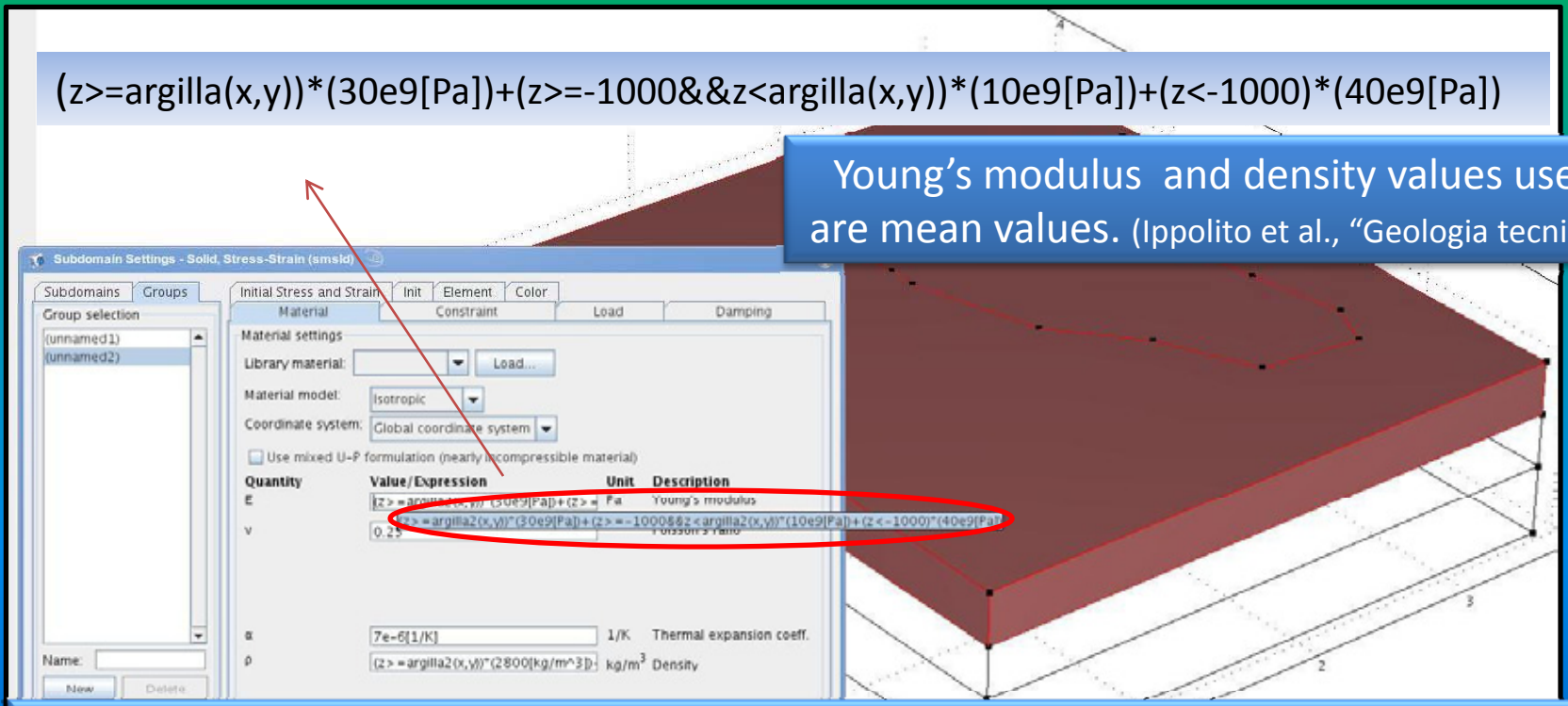

Young's modulus and density values used are mean values. (Ippolito et al., "Geologia tecnica")

From -1km to -10 km we put mostly carbonatic succession and crystalline rocks, grouped as a unique physical group with intermediate characteristics .

2002 Eruption as seen with FEM

Subdomain settings

Gravitational load application

the gravitational load application is parametrized by the use of the parameter *para* that goes from 0 to 2 with a step of 0.1. The gravitational load is gradually applied when para is <1 and is maintained to its 100% for 1<para<2

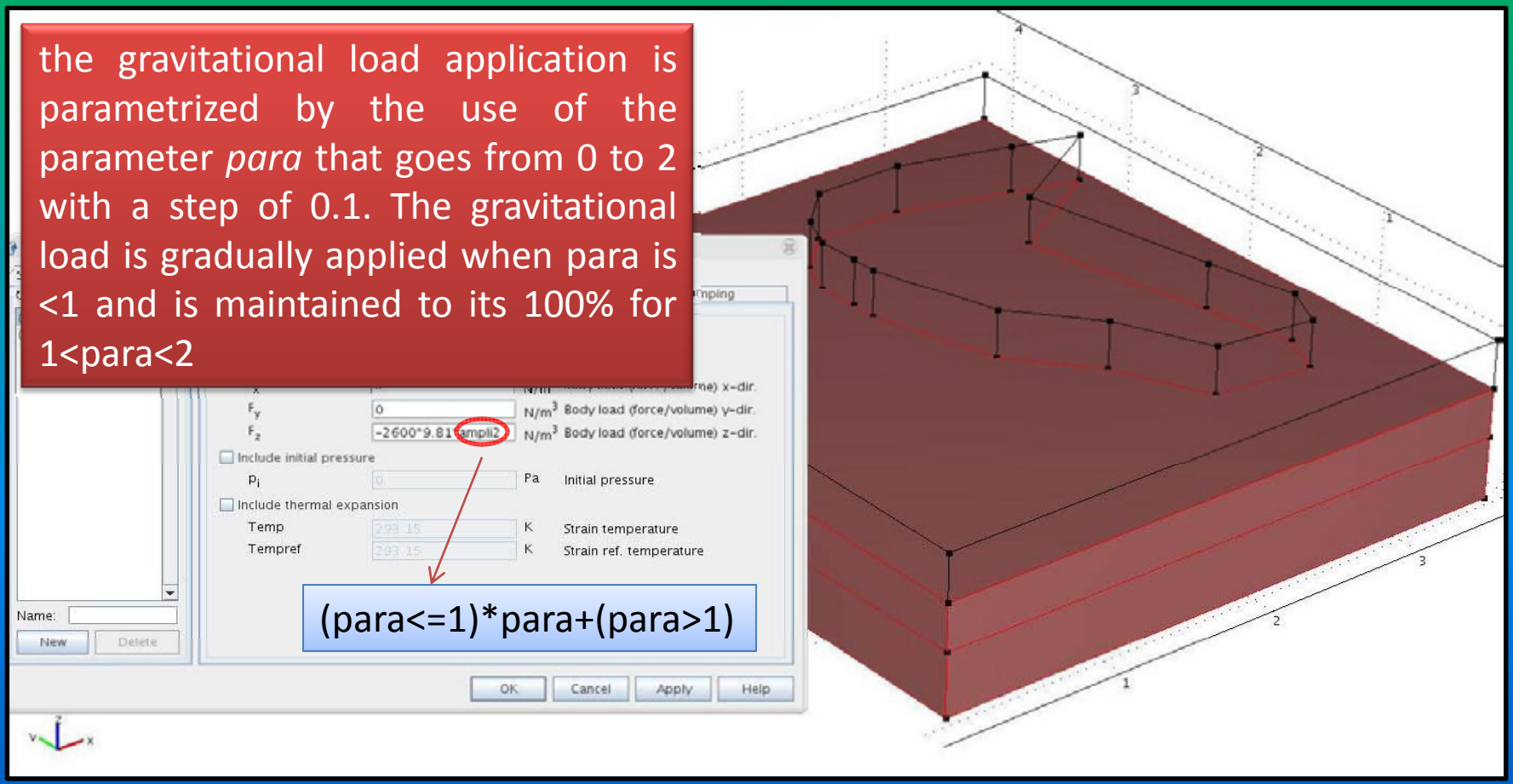

2002 Eruption as seen with FEM

Boundary settings

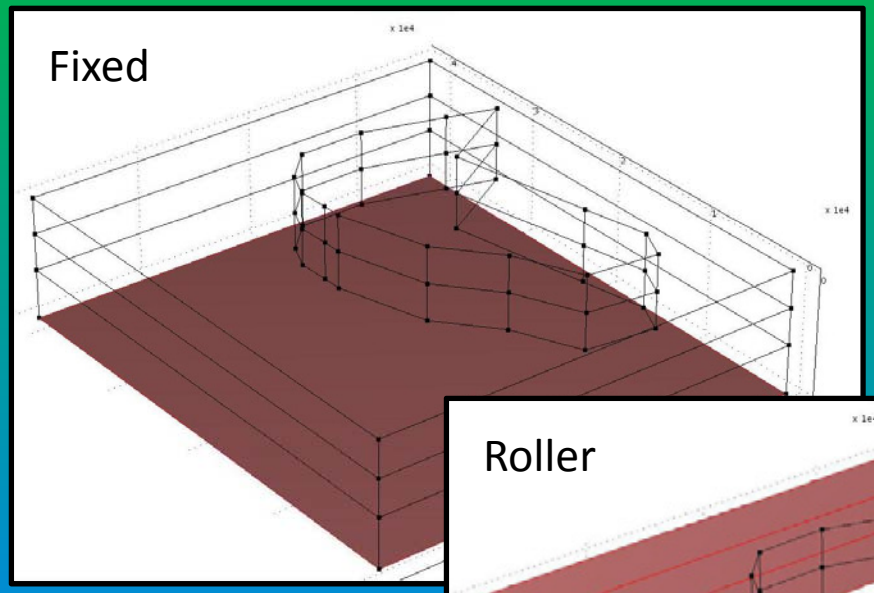

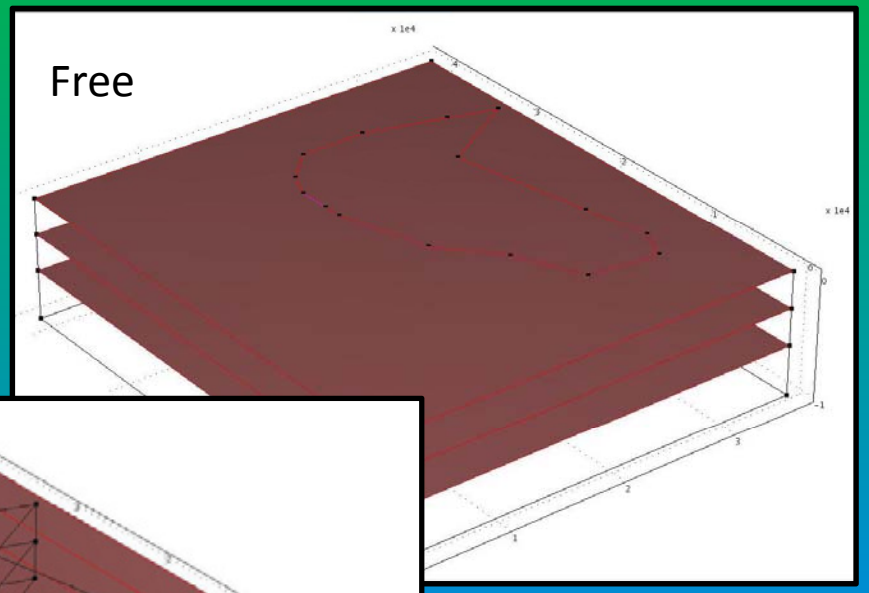

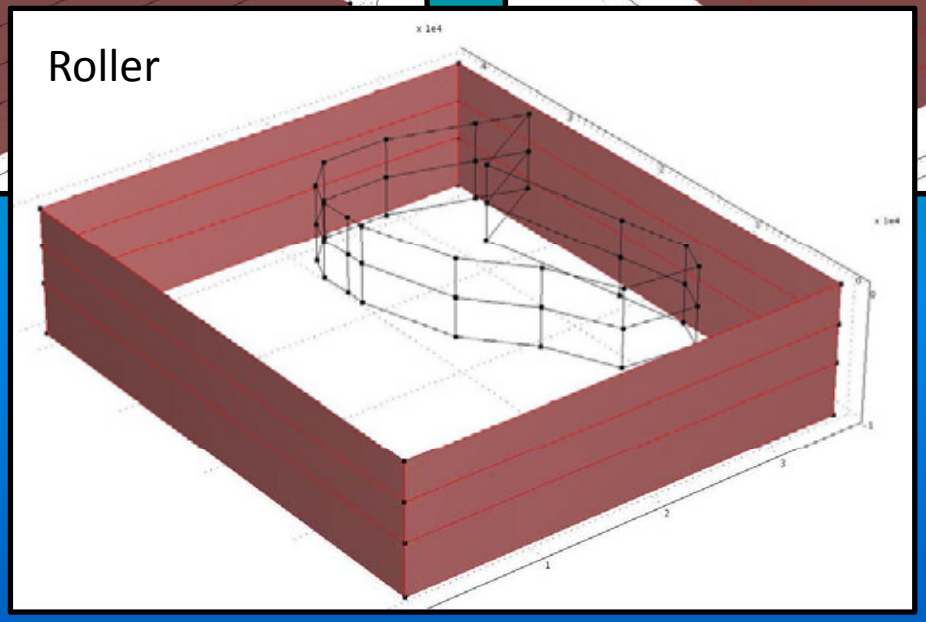

2002 Eruption as seen with FEM

Boundary settings

North dike I

((z>=-2000)*(spost2)+(z<-2000)*(spost1))*ampli
0.5 m Shear component

-((z>=-2000)*(spost)+(z<-2000)*(spost1))*ampli
1 m Opening component

ampli:(para>1)*(-1+para)

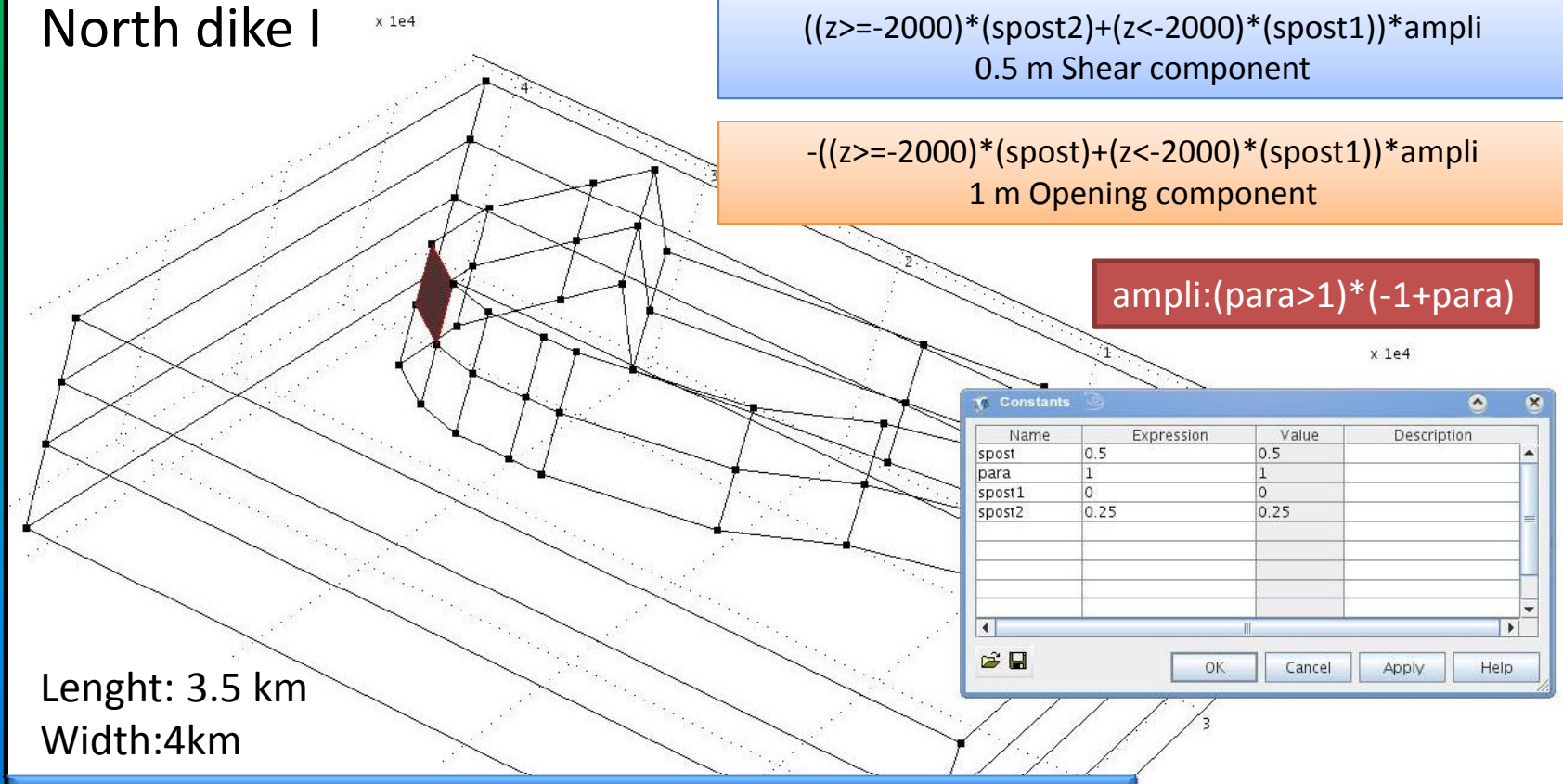

Lenght: 3.5 km
Width:4km

The minus sign indicates that the movement is applied to the outgoing normal.

2002 Eruption as seen with FEM

Boundary settings

North dike II

-((z>=-2000)*(spost)+(z<-2000)*(spost1))*ampli
1 m opening Component

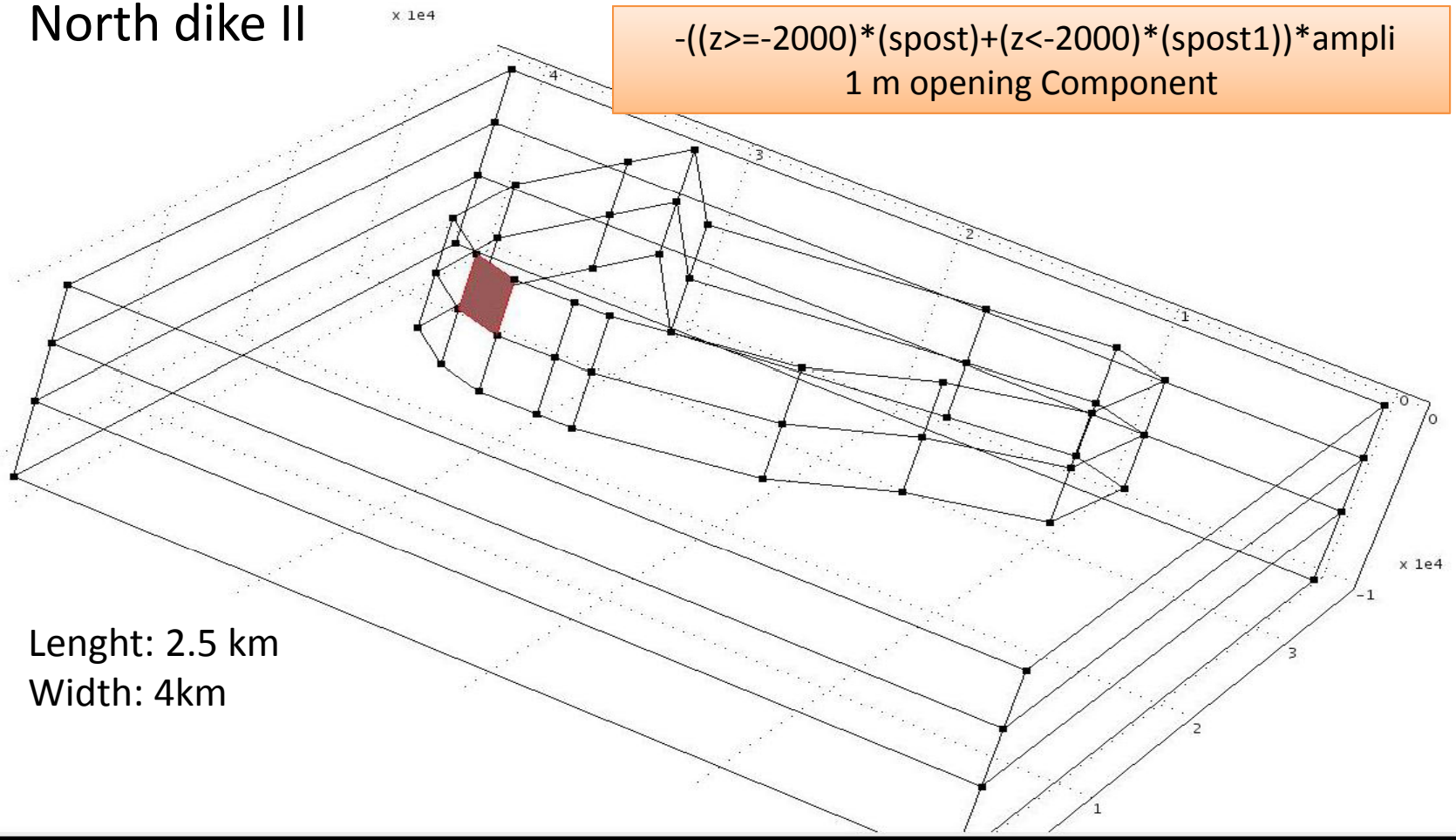

Lenght: 2.5 km
Width: 4km

2002 Eruption as seen with FEM

Boundary settings

South dike

-((z>=-500)*(spost)+(z<500)*(spost1))*ampli
1 m Opening Component

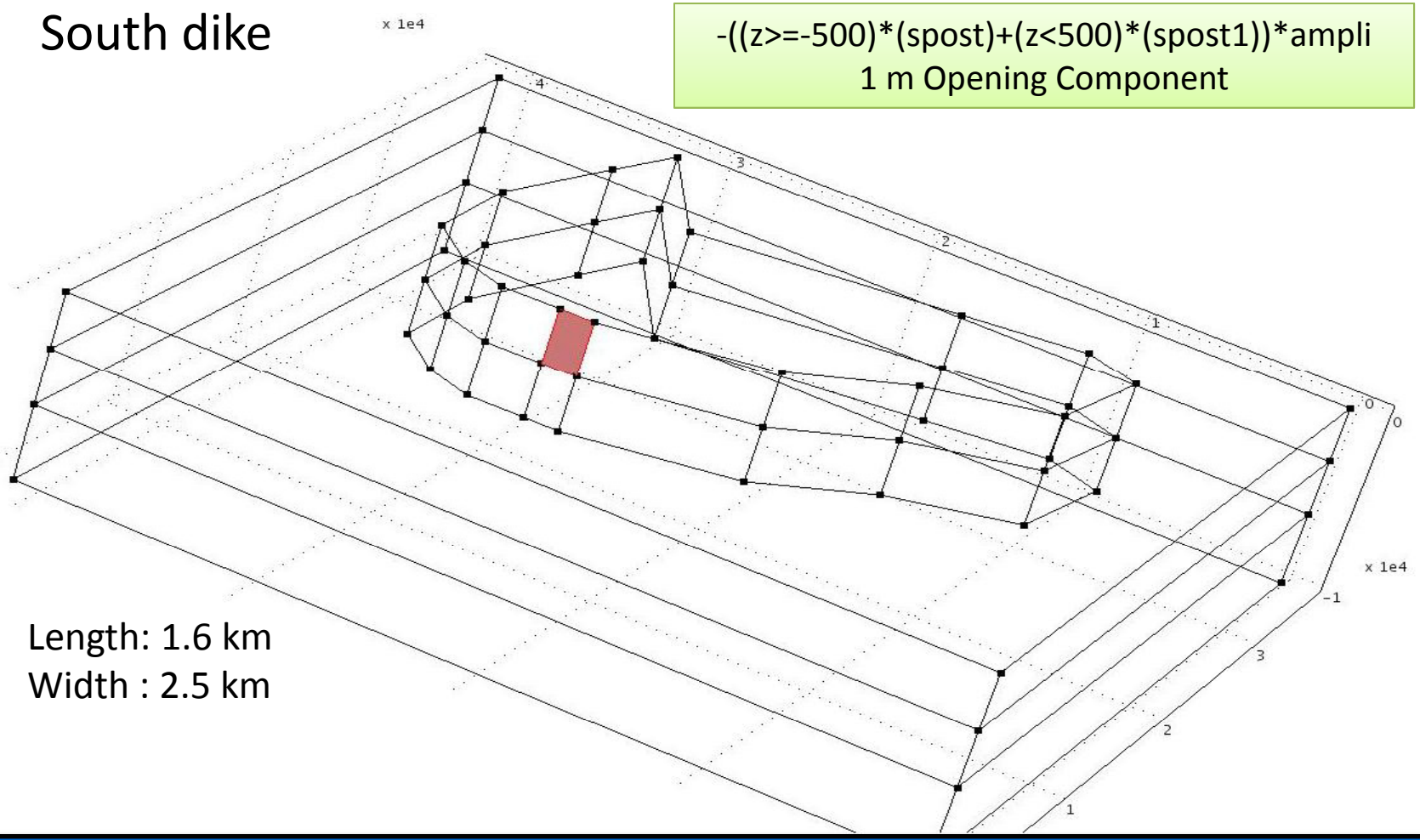

Length: 1.6 km
Width : 2.5 km

2002 Eruption as seen with FEM Boundary settings

Using *contact pairs* four fault systems have been inserted. Each fault plane is formed by a couple of boundaries simulating the two blocks that can dislocate: master boundaries are light blue while slave boundaries are purple).

Contact pairs have an initial contact pressure and can separate or slide each other but no compenetration is possible.

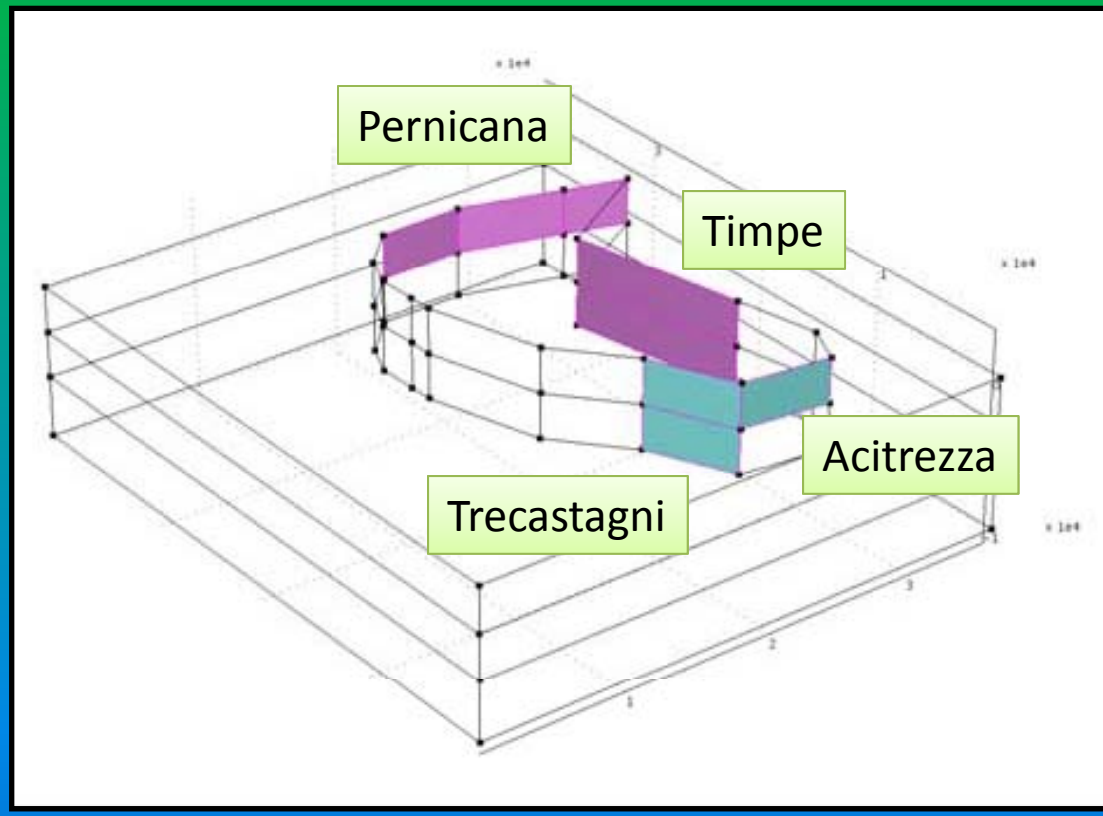

Fault planes position has been inferred from geological and structural data available in literature and directly mapped in the field, the fault planes depth has been established from earthquakes hypocentral distribution (Patanè et al., 2005). Pernicana and Acitrezza depth is -3 km. Timpe and Trecastagni depth is -6km.

2002 Eruption as seen with FEM

Mesh generation

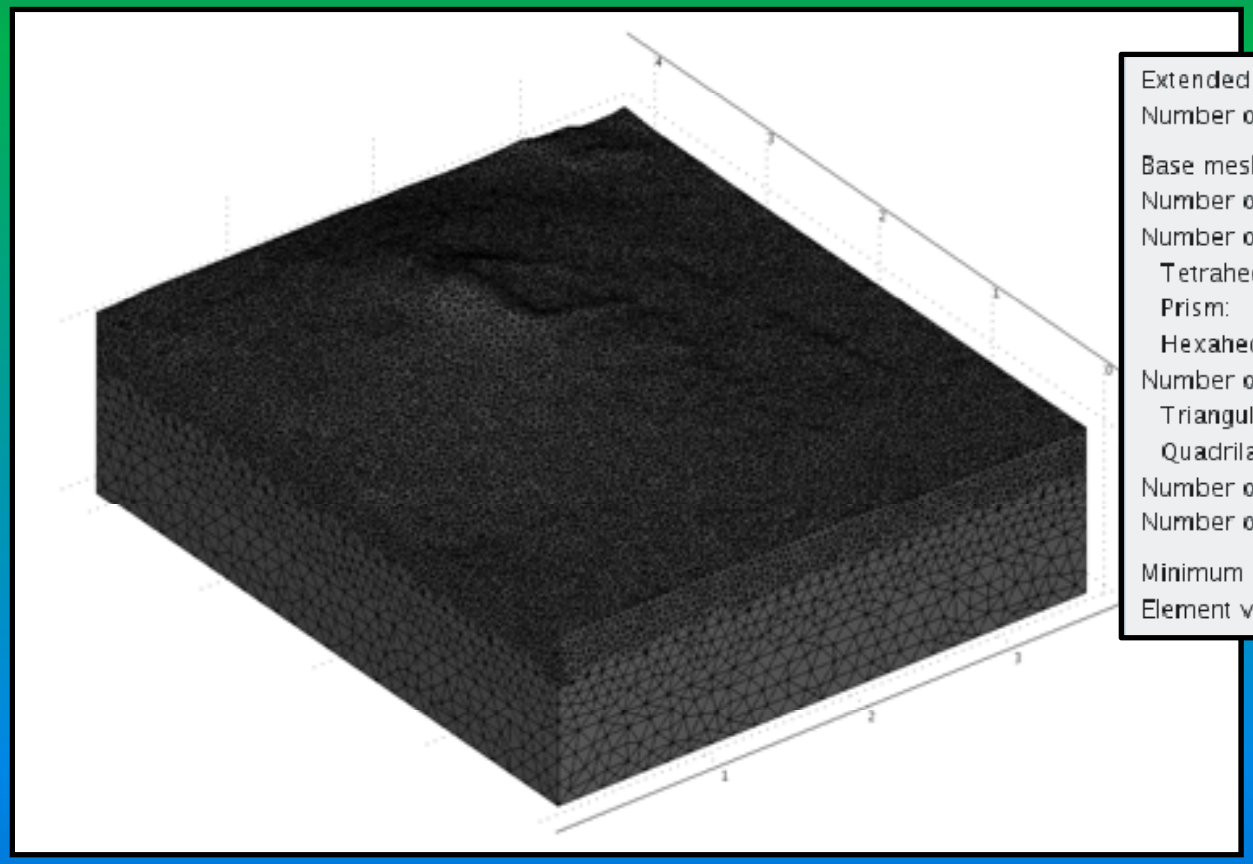

Extended mesh:	
Number of degrees of freedom:	427261
Base mesh:	
Number of mesh points:	141929
Number of elements:	781543
Tetrahedral:	781543
Prism:	0
Hexahedral:	0
Number of boundary elements:	70419
Triangular:	70419
Quadrilateral:	0
Number of edge elements:	2060
Number of vertex elements:	106
Minimum element quality:	0.2535
Element volume ratio:	0.0028

The mesh is gradually refined from bottom (maximum element size 1500) to top (maximum element size 500), where more accuracy is required. The number of degrees of freedom is about 400 thousand.

Solving settings

The model is solved with a parametric solver (PARDISO) in three phases:

For *para = 0* all the conditions applied are controlled

For 0<*para*<1 the gravitational load is gradually applied.

For *para*>1 the gravitational load is maintained to its 100% and prescribed displacements of the dikes are gradually applied until the simulation ends at *para*=2

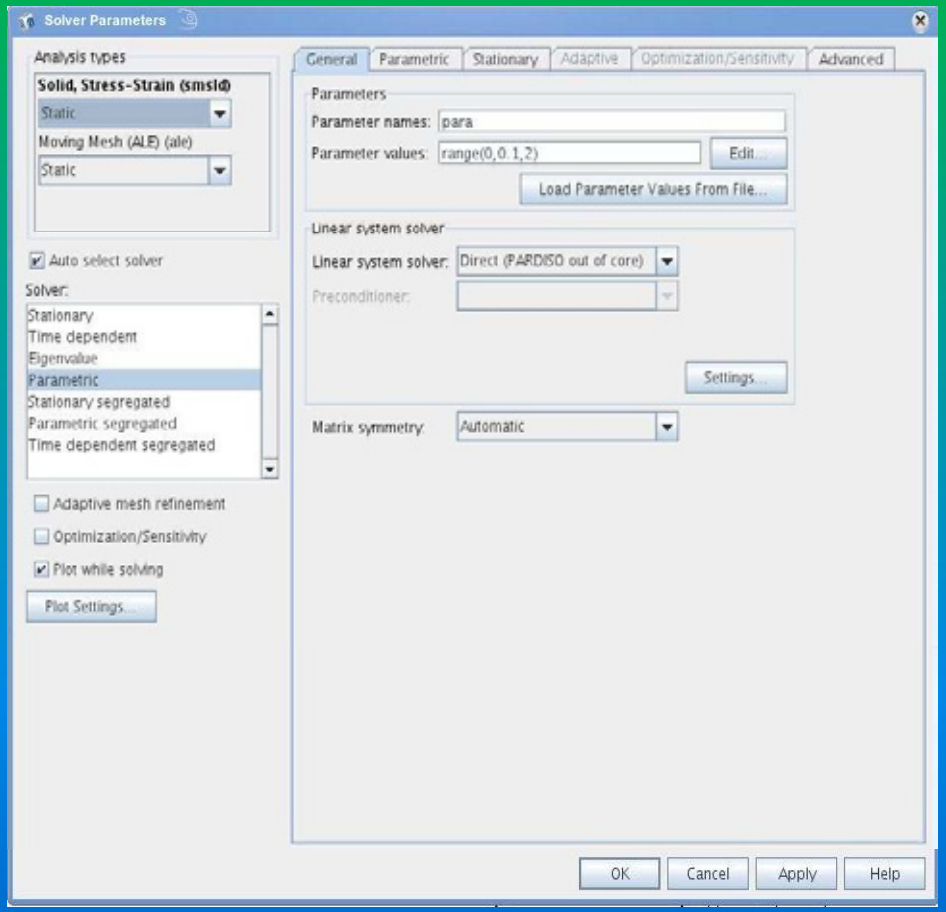

Results

We are interested to know x,y and z ground displacements as triggered by the dikes.

x , y and z values can be get, plotting the following expressions:

u-with(11,u)

v-with(11,v)

w-with(11,w)

u , v, w are the variables for represent x, y and z displacements

11 is the eleventh step of para (para=1) when the maximum value of gravitational load is reached

with is a special function to subtract the gravitational load.

The abrupt gravitational load application leads to an overall lowering of the volcano and of the other layers. This effect is not present in the real situation where (for short times) an equilibrium state can be considered.

Results

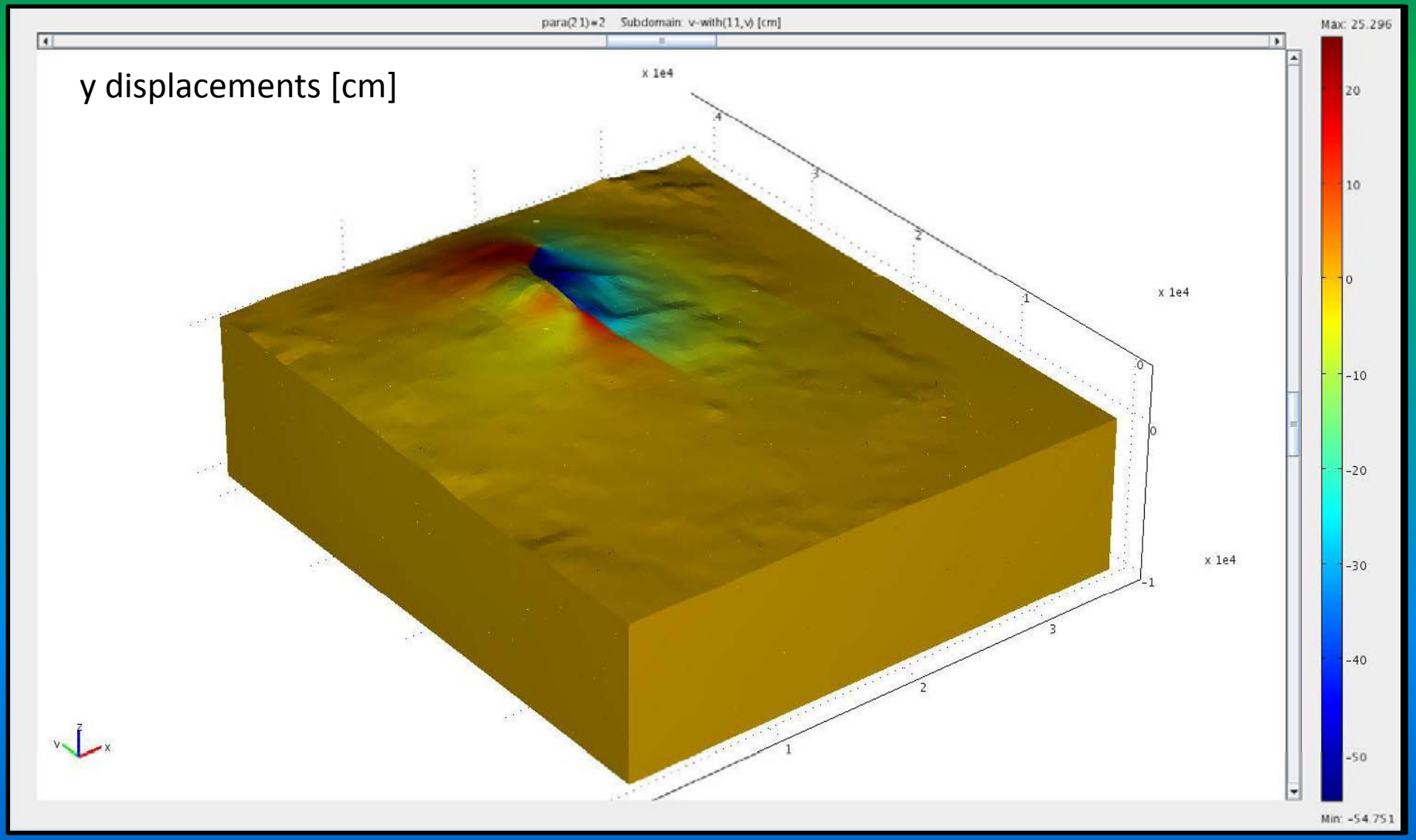
para(21)=2 Subdomain: v-with(11,v) [cm]
y displacements [cm]
x 1e4
x 1e4
x 1e4
Max: 25.296
20
10
0
-10
-20
-30
-40
-50
Min: -54.751

Results

Recorded,FEM and analytical x-y vectors

Good agreements between recorded and FEM data can be seen at Monte Gallo (EMGL), Monte Egitto (EMEG) and Monte Fontana (EMFN).

At Monte Maletto (EMAL) station FEM and recorded vectors have similar modulus but different orientations;

Serra La Nave (ESLN) and Nicolosi (NICO) orientation and versus are similar to analytical;

At Monte Farelle (EFAR), FEM vector orientation is similar to recorded but the modulus of FEM and analytical vectors are double respect to recorded one.

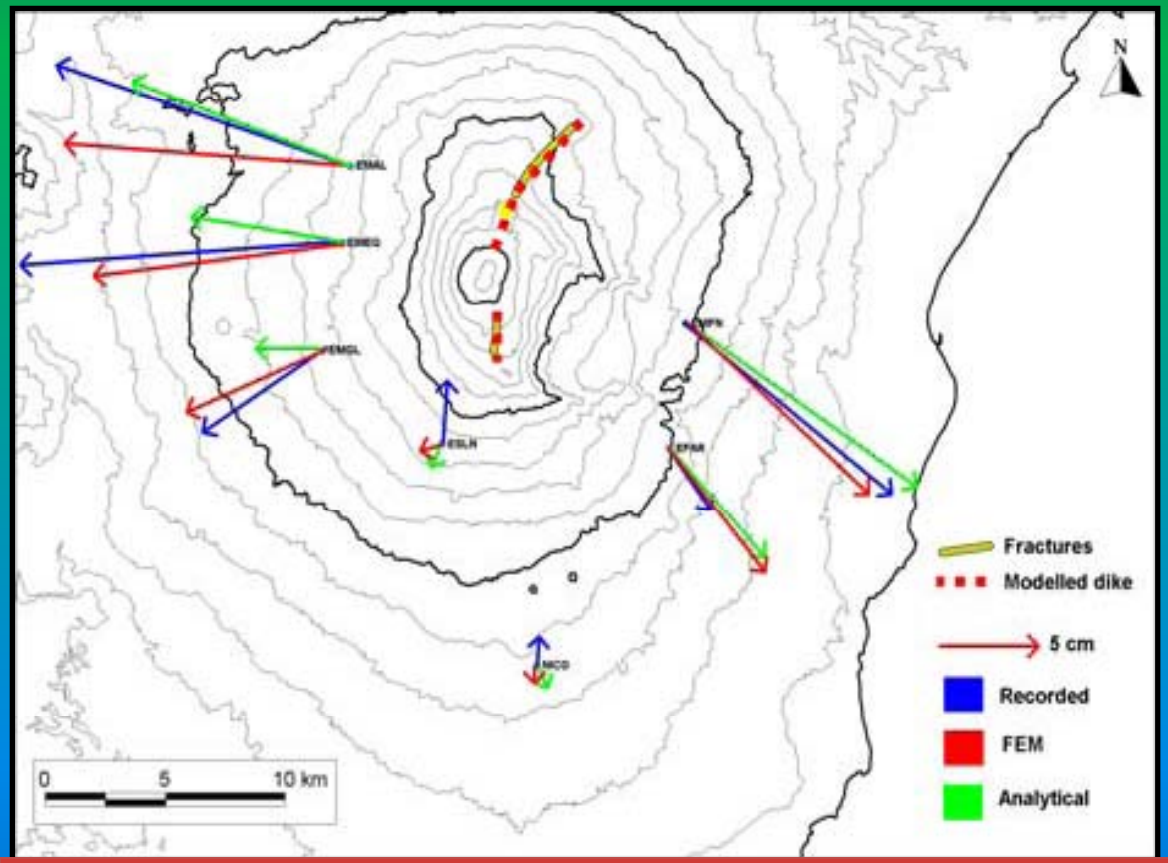

Comparison between displacement vectors at GPS stations as estimated from recorded, numerical, and analytical data (Aloisi et al., 2003)

Results

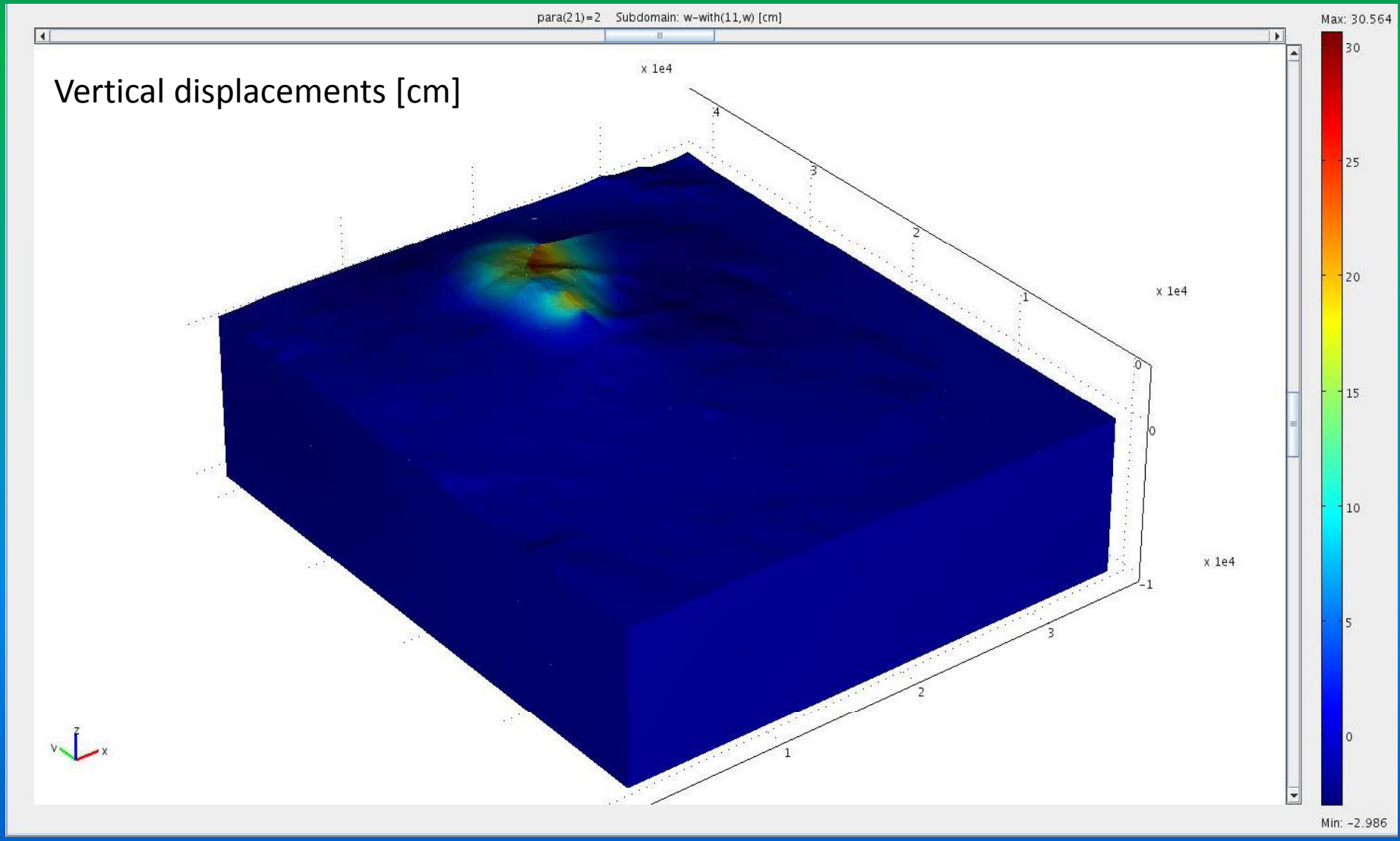
para(21)=2 Subdomain: w-with(11,w) [cm]
Vertical displacements [cm]
x 1e4
x 1e4
x 1e4
Max: 30.564
30
25
20
15
10
5
0
Min: -2.986

Results

Recorded,FEM and analytical vertical displacements

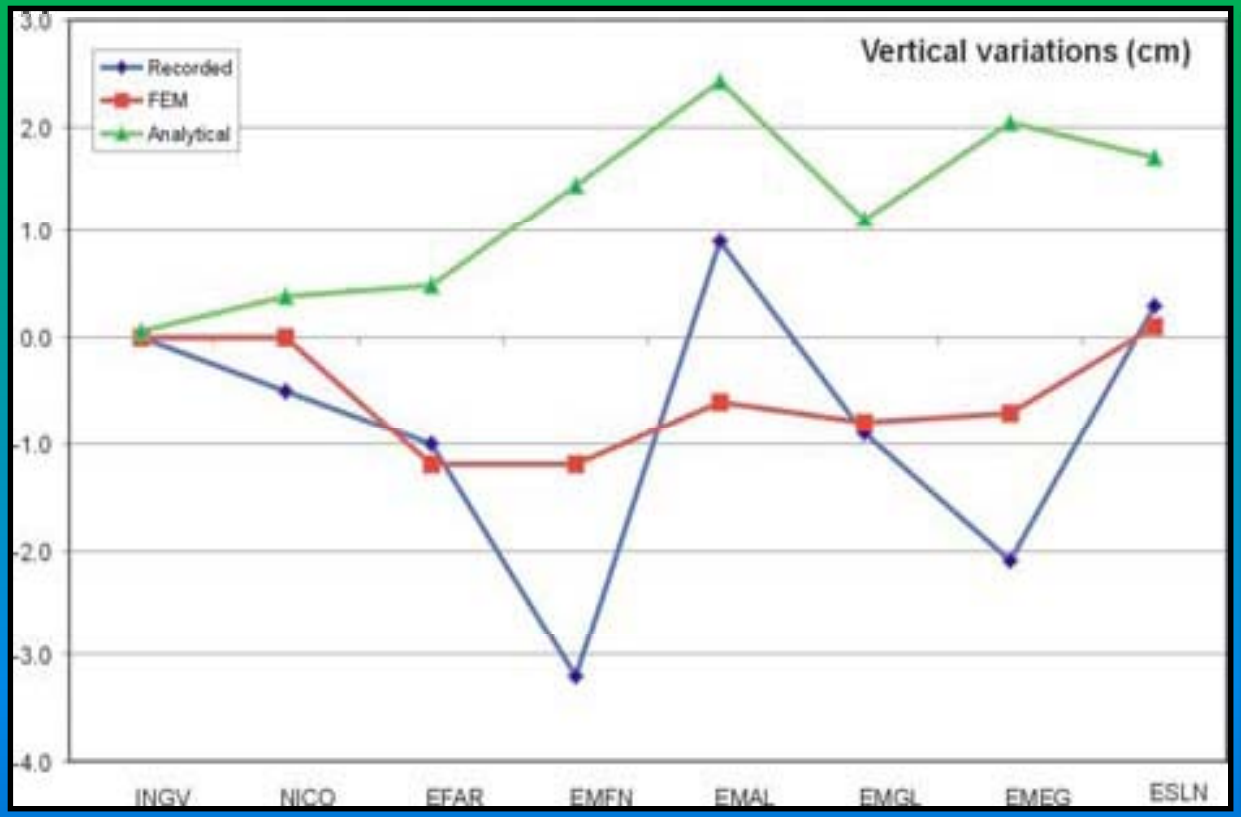

Comparison between recorded, FEM and analytical vertical variations.

FEM approach explains vertical variations better than analytical approach in almost all stations because it is able to compute also negative vertical variations. Analytical approach gives instead positive values only. The only difference is at EMAL where FEM gives a negative value respect to the positive value recorded.

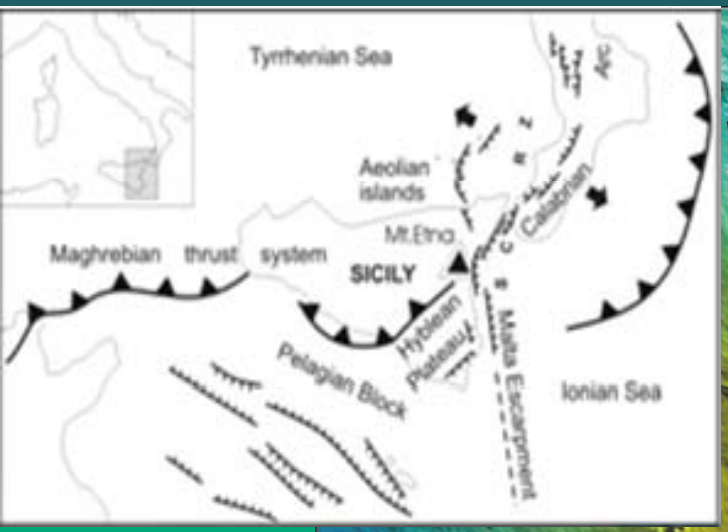
Tyrrhenian Sea
Aeolian islands
Mt.Etna
Maghrebian thrust system
SICILY
Hyblean Plateau
Malta Escarpment
Calabrian Arc
Pelagian Block
Ionian Sea

Randazzo
Linguaglossa
Piedimonte Etneo
Pernicana fault
NE Rift Zone
SW-NE system
Summit Craters
SE Crater
Valle del Bove
La Montagnola
S Rift Zone
NNW-SSE system
Adrano
S. Alfio
Giarre
Timpe fault system
Zafferana
S. Venerina
Mascalucia-Trecastagni system
Acireale
Aci trezza fault
Acicastello
CATANIA
Normal fault (arrow indicates horizontal component of motion)
Strike-slip fault
Presumed fault
Eruptive fissure
Valle del Bove rims
N
0
5
10 km

x displacements along Pernicana fault

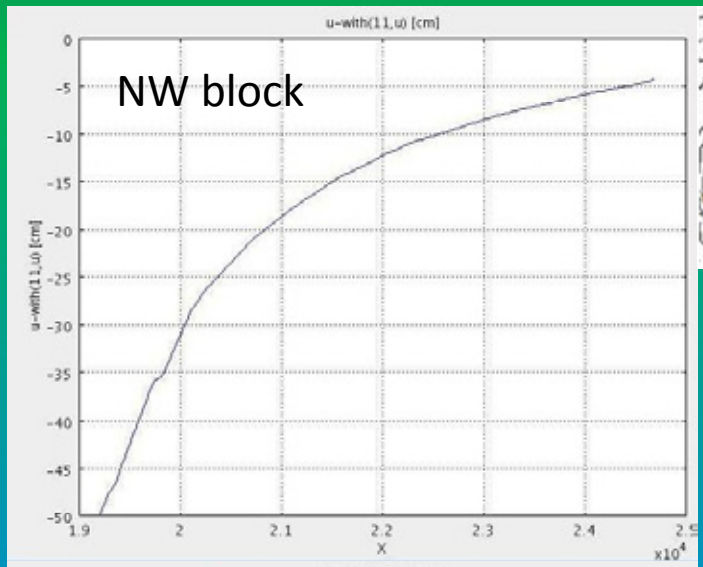

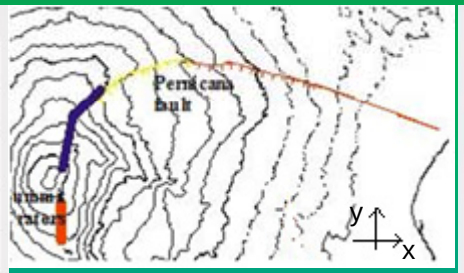

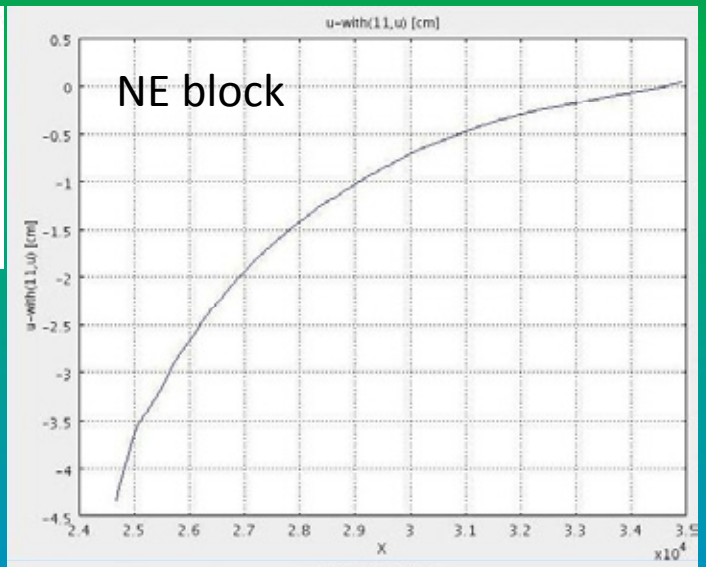

Left-lateral strike slip

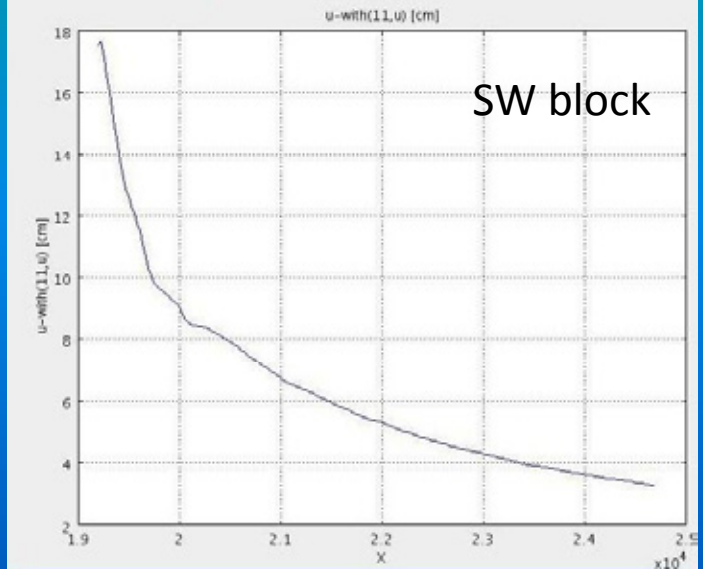

y displacements along Pernicana fault

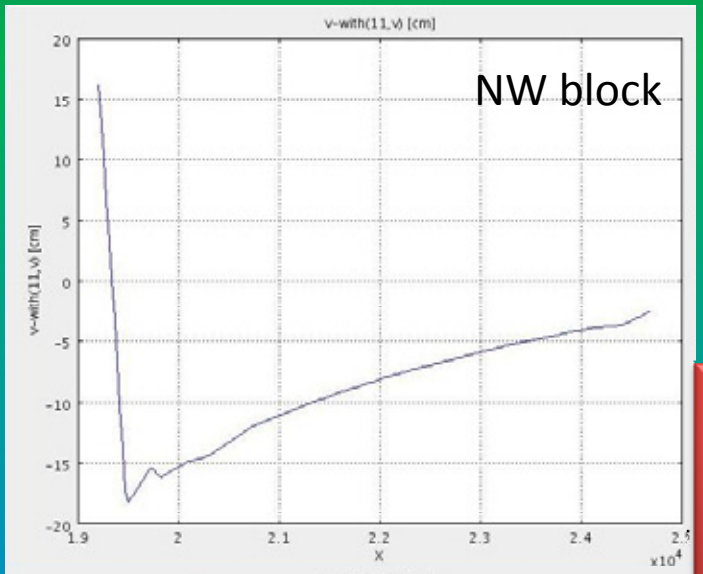

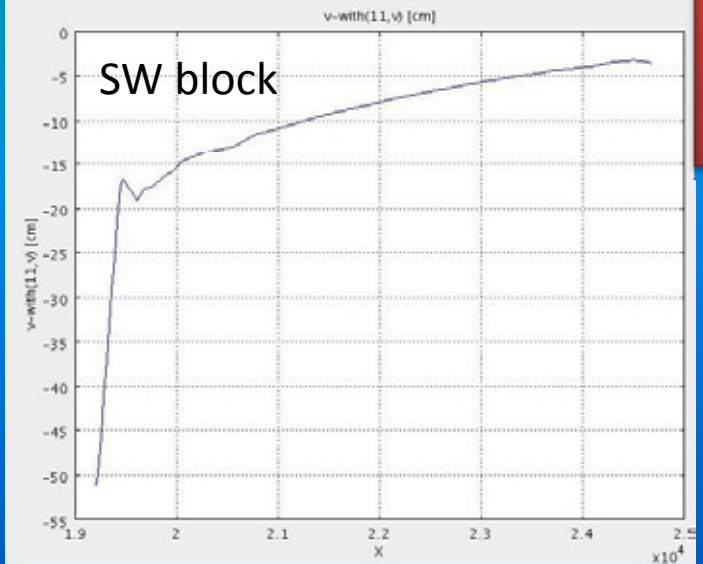

xy vectors gradually rotate (from N45W to N100W at north and from N135E to N100E until they are parallel to the fault plane

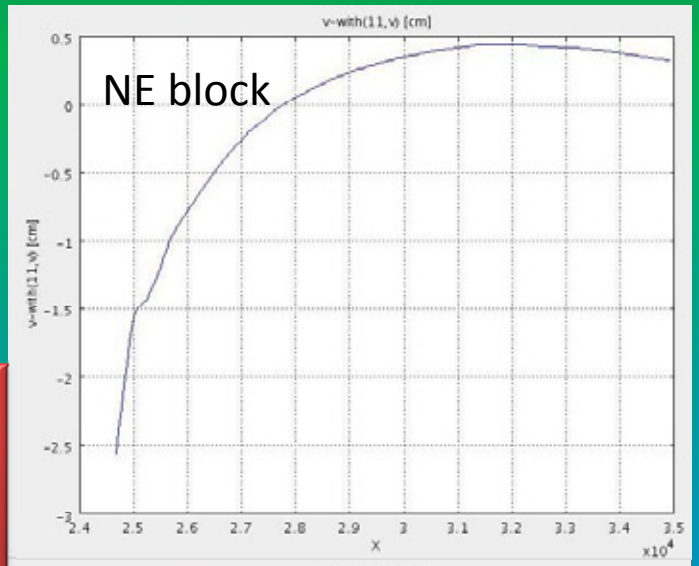

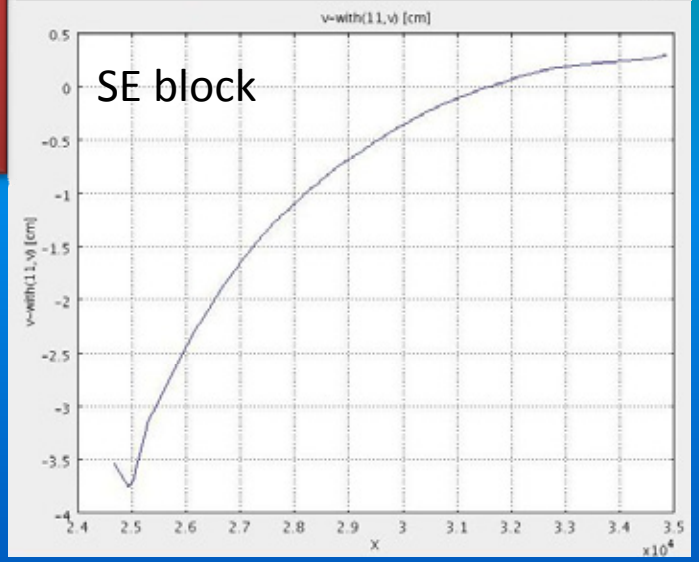

z displacements along Pernicana fault

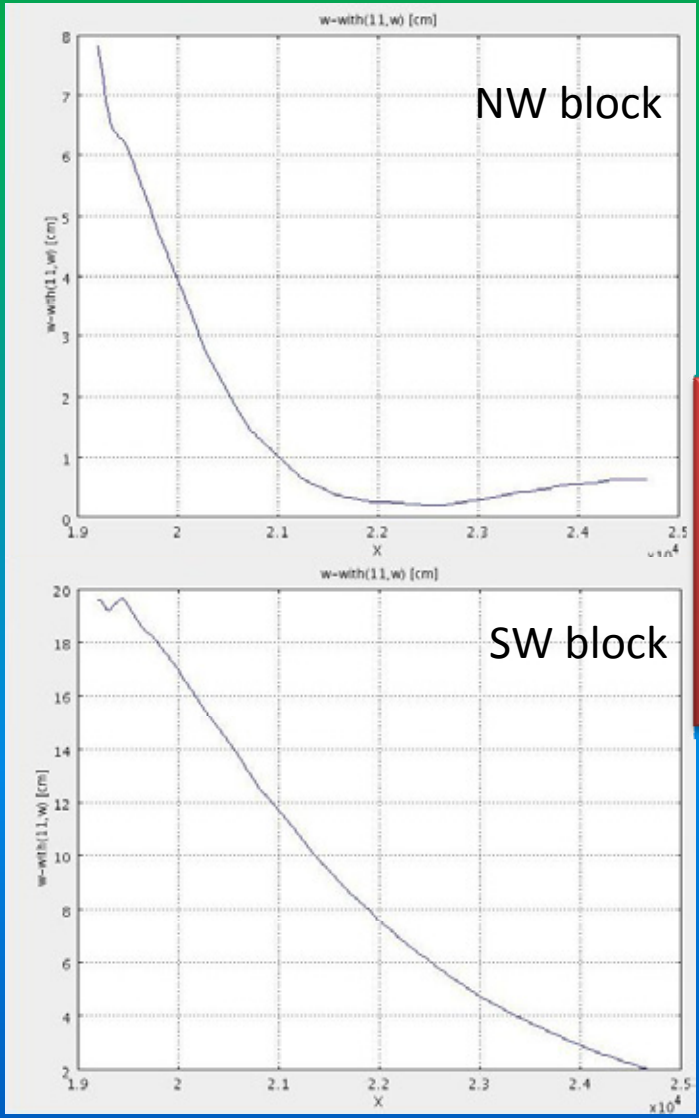

The southern block has a major vertical motion respect to the northern one. It goes rapidly to zero proceeding eastwards

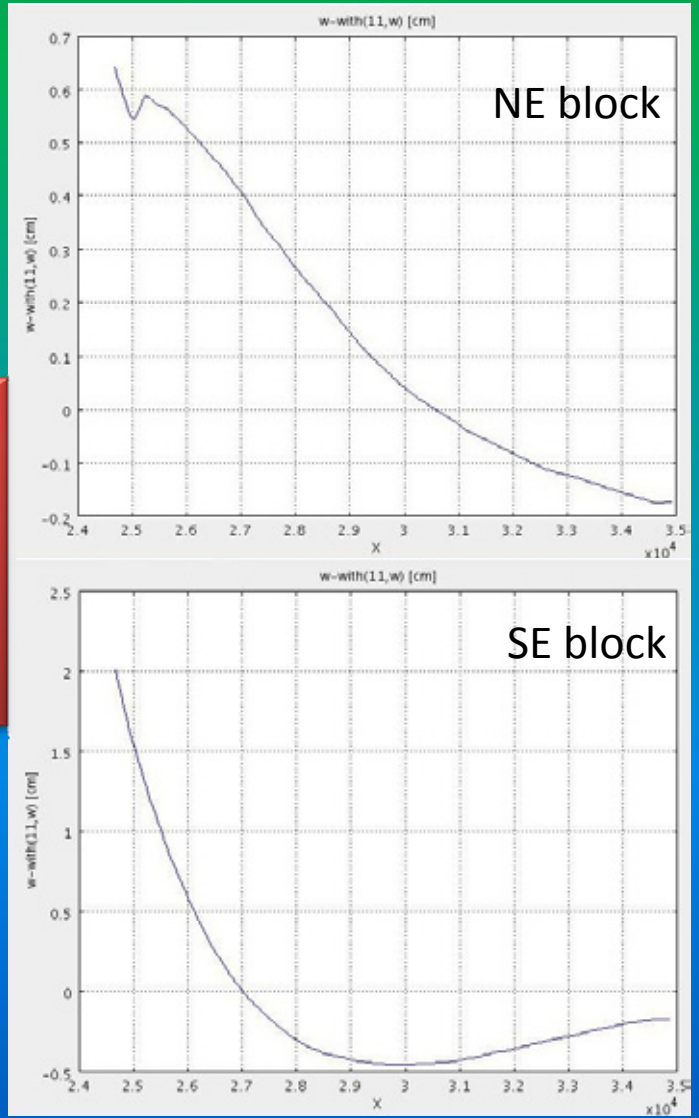

x and y displacements along Timpe fault system

x

left lateral strike slip

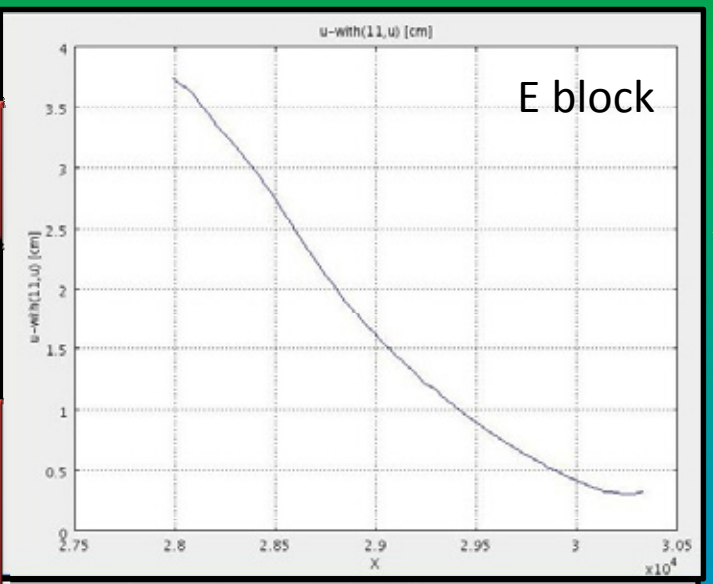

x

On west side vectors oriented N135E gradually rotate to N170E

y

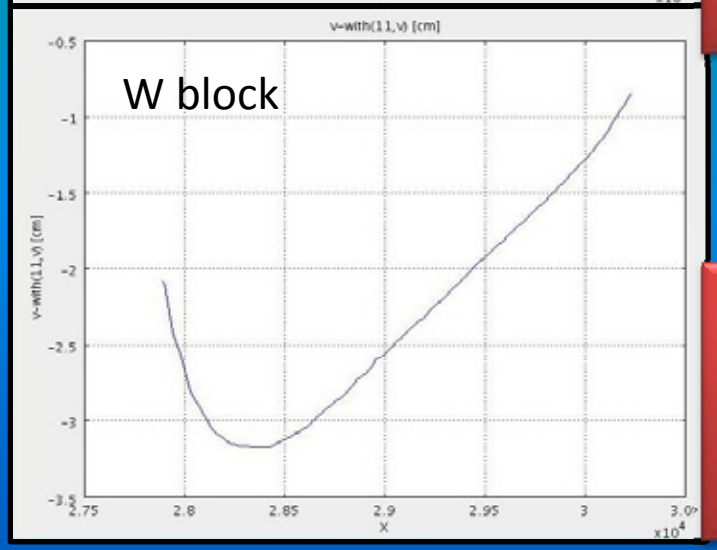

On east side vectors are oriented N90E and gradually rotate N170E aligning with fault

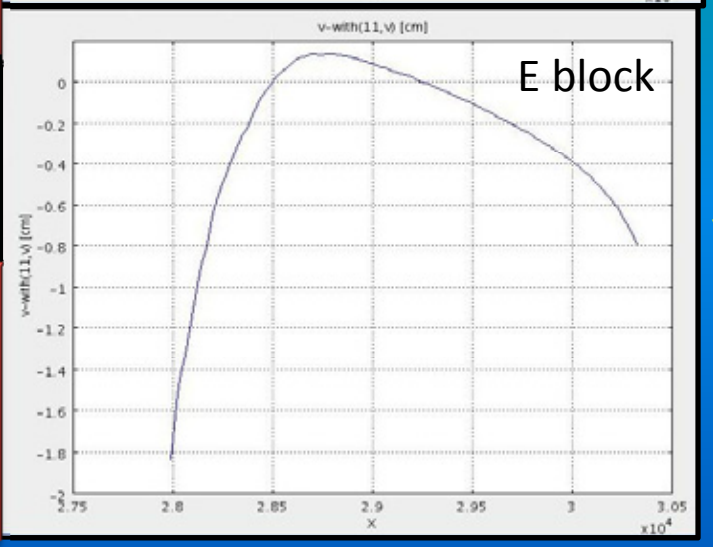

y

z displacements along Timpe fault system

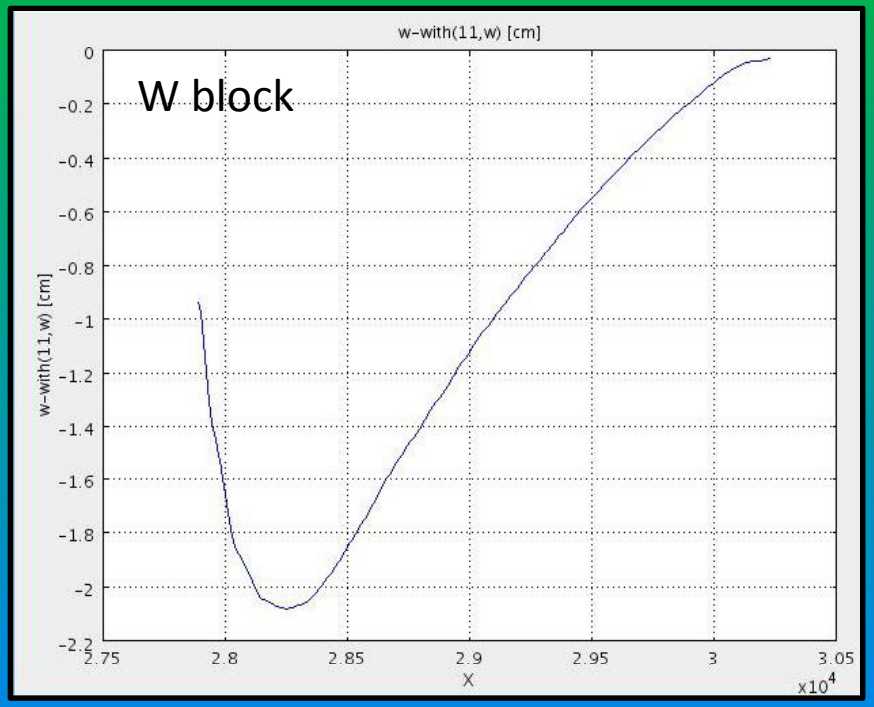

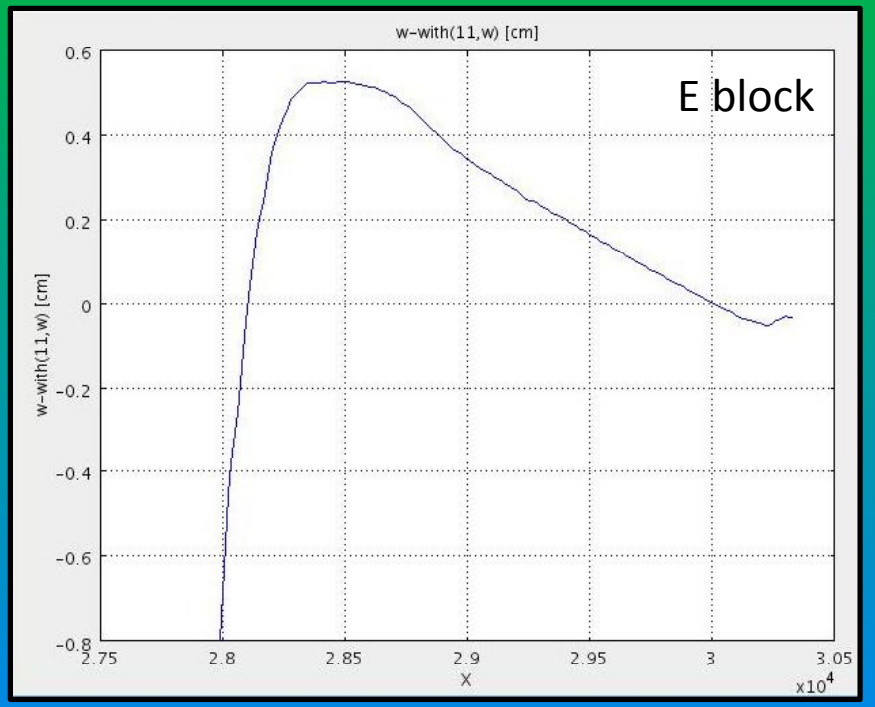

Vertical variation shows a lowering on the west side and in the northern part of the east side. At west the lowering reaches -2 cm and then goes smoothly to -0.1 towards south. At east the downlift goes rapidly to zero and becomes an uplift of 0.5 cm then it goes smoothly to zero again.

x and y displacements along Trecastagni fault

x

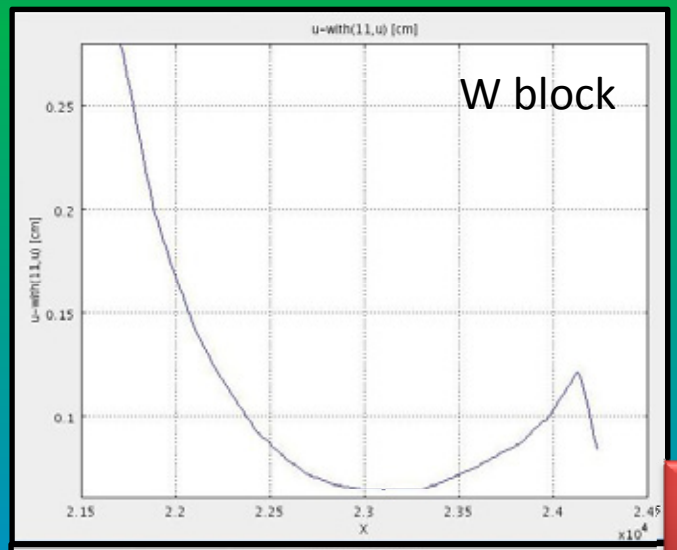

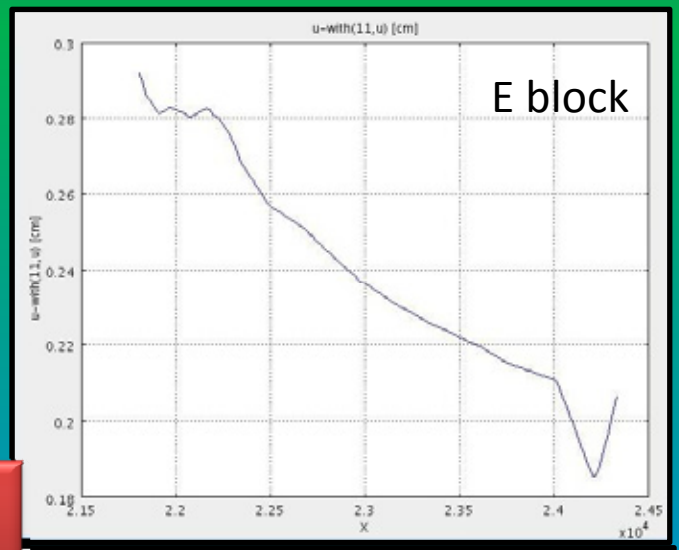

x

Right lateral strike- slip

y

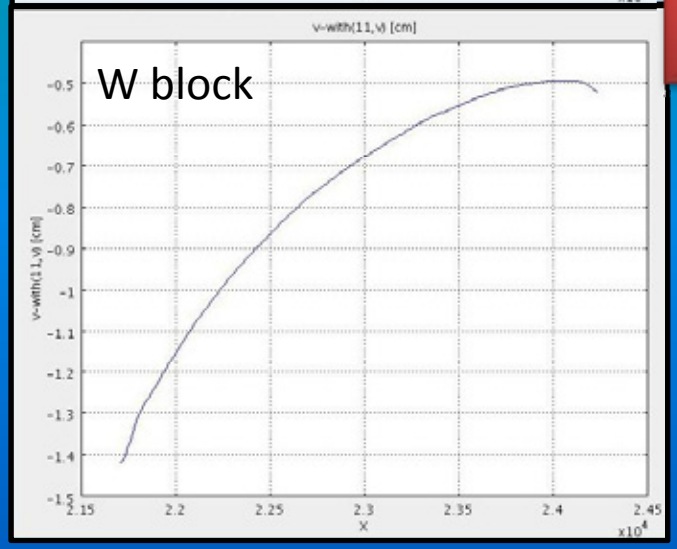

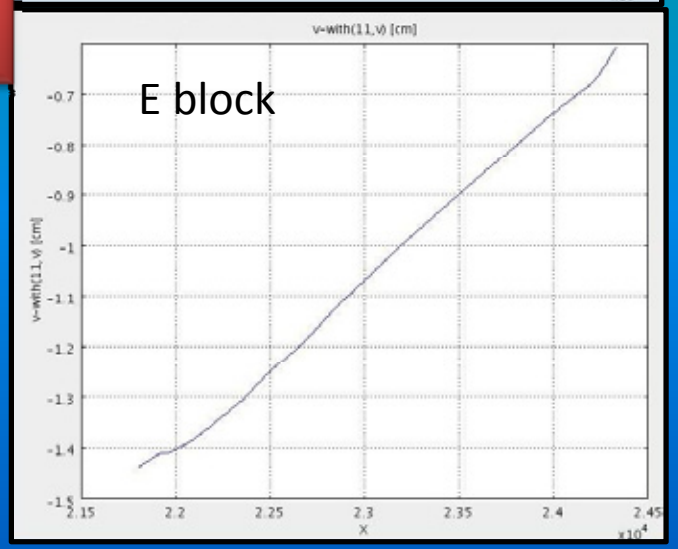

y

z displacements along Trecastagni fault

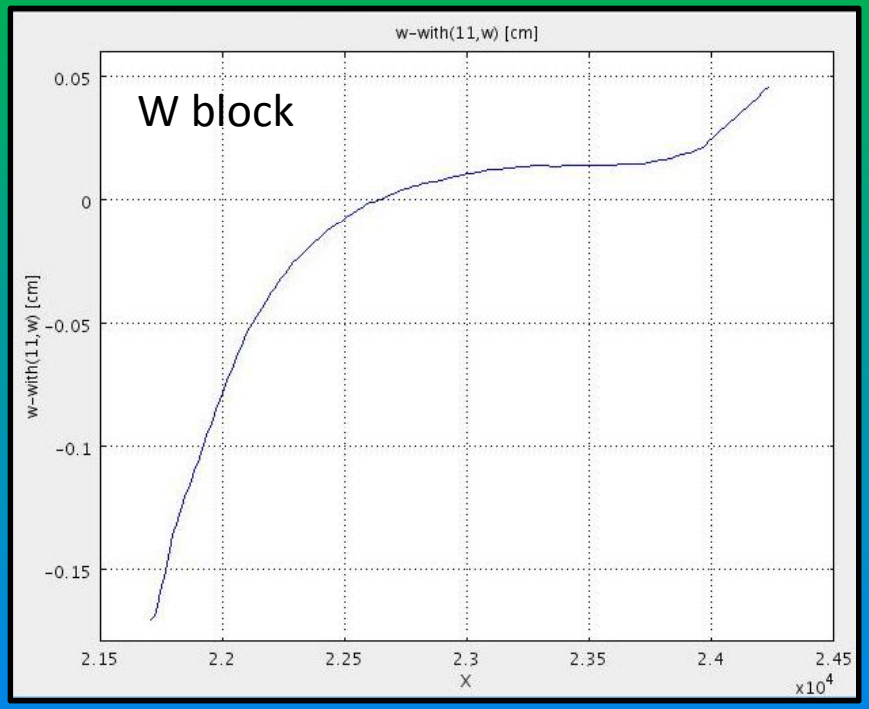

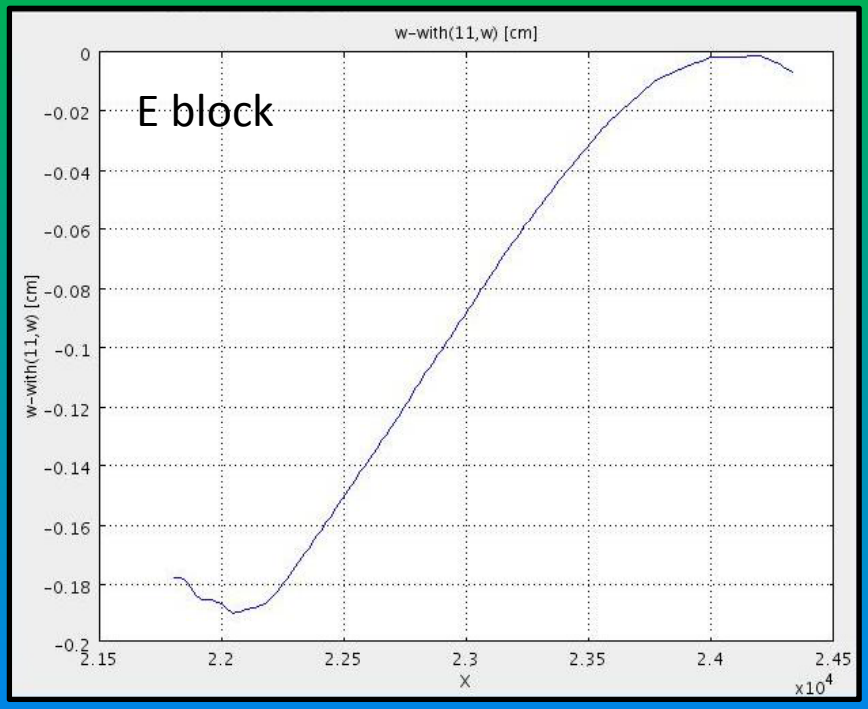

z displacements show a lowering on the northwest and northeast sides of -0.18 cm rapidly going to zero southwards. A very little uplift is present at the southwest side probably for the contact with Acitrezza fault.

x and y displacements along Acitrezza fault

x

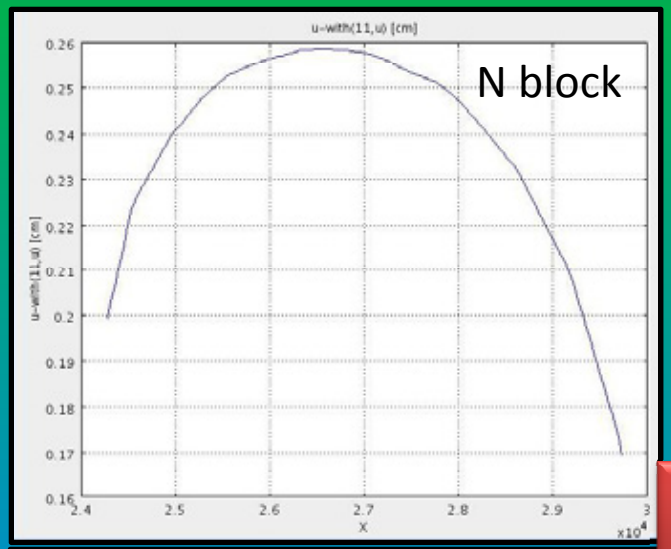

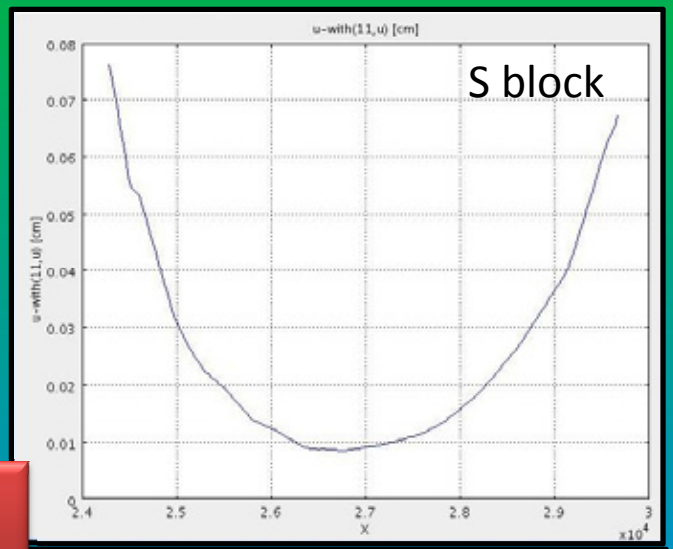

x

right lateral strike slip

y

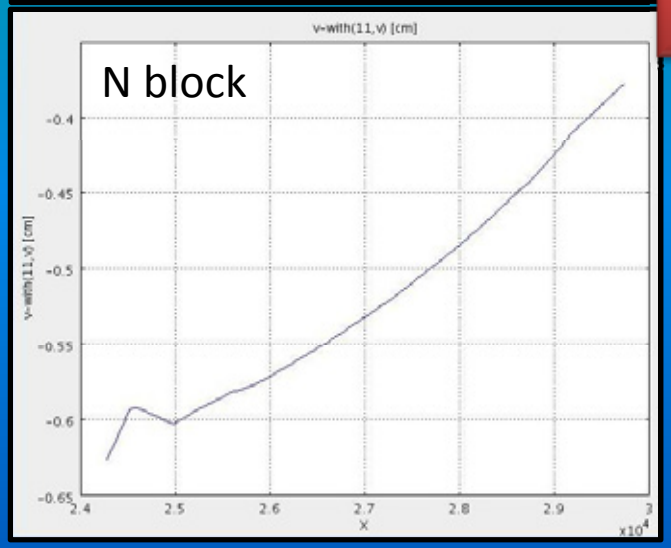

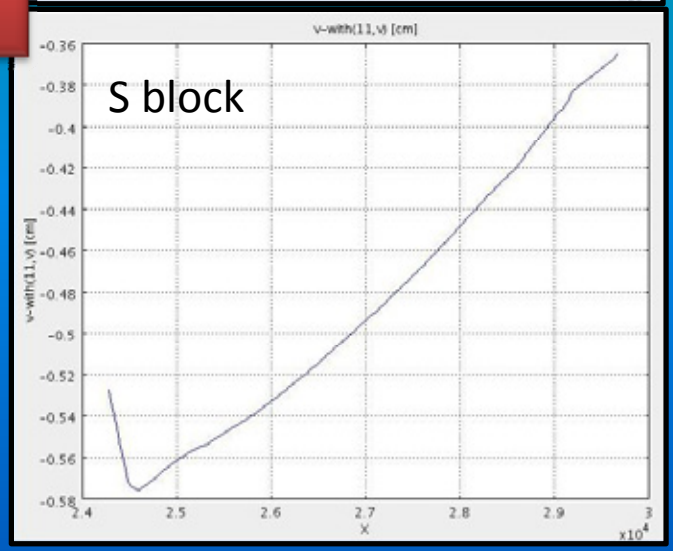

y

z displacements along Acitrezza fault

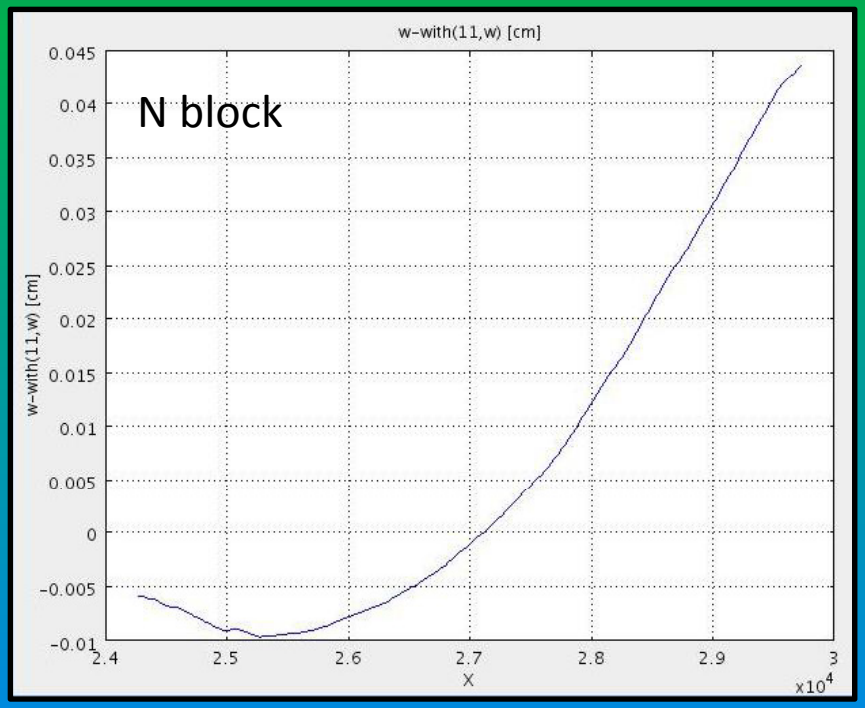

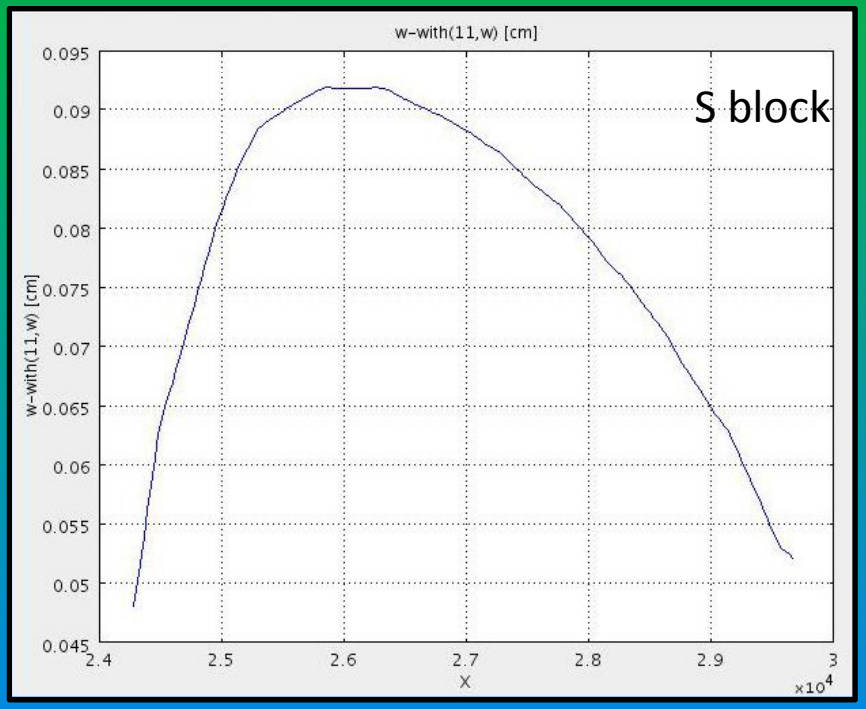

z displacements show a very small initial lowering in the northwest part evolving gradually to a little uplift. On the south side a little uplift rapidly grows up until it reaches a maximum value of about 0.09 cm and then rapidly decreases going eastwards.

Reduced chi-squared X2 has been carried out

The reduced chi-squared X2 for FEM data is equal to 1.0 considering an a-posteriori standard deviation of 0.018 m for the horizontal and vertical displacements. Otherwise with the same standard deviation the analytical model is not able to pass the reduced chi-square test; to pass it, the a-posteriori standard deviation must be 0.030 m

Coulomb stress variations on Timpe fault system

Change of Coulomb stress for right-lateral motion on planes orientated at ψ with respect to the x-axis:

Simpson and Reasenberg(1994)]

$$\sigma_f^R = \tau_{13}^R + \mu' \sigma_{33}$$

$$\sigma_{33} = \sigma_{xx}\sin^2\psi - 2\sigma_{xy}\sin\psi\cos\psi + \sigma_{yy}\cos^2\psi$$

$$\tau_{13} = \frac{1}{2}(\sigma_{yy}-\sigma_{xx})\sin 2\psi + \tau_{xy}\cos 2\psi$$

μ‘=μ(1-B)

0<B<1= Skempton’s Coefficient

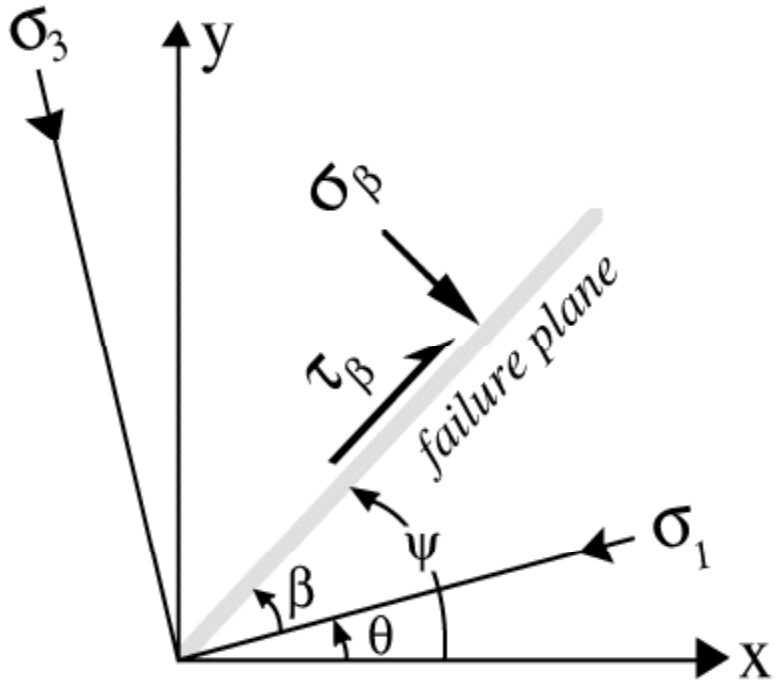

[King et al., 1994]

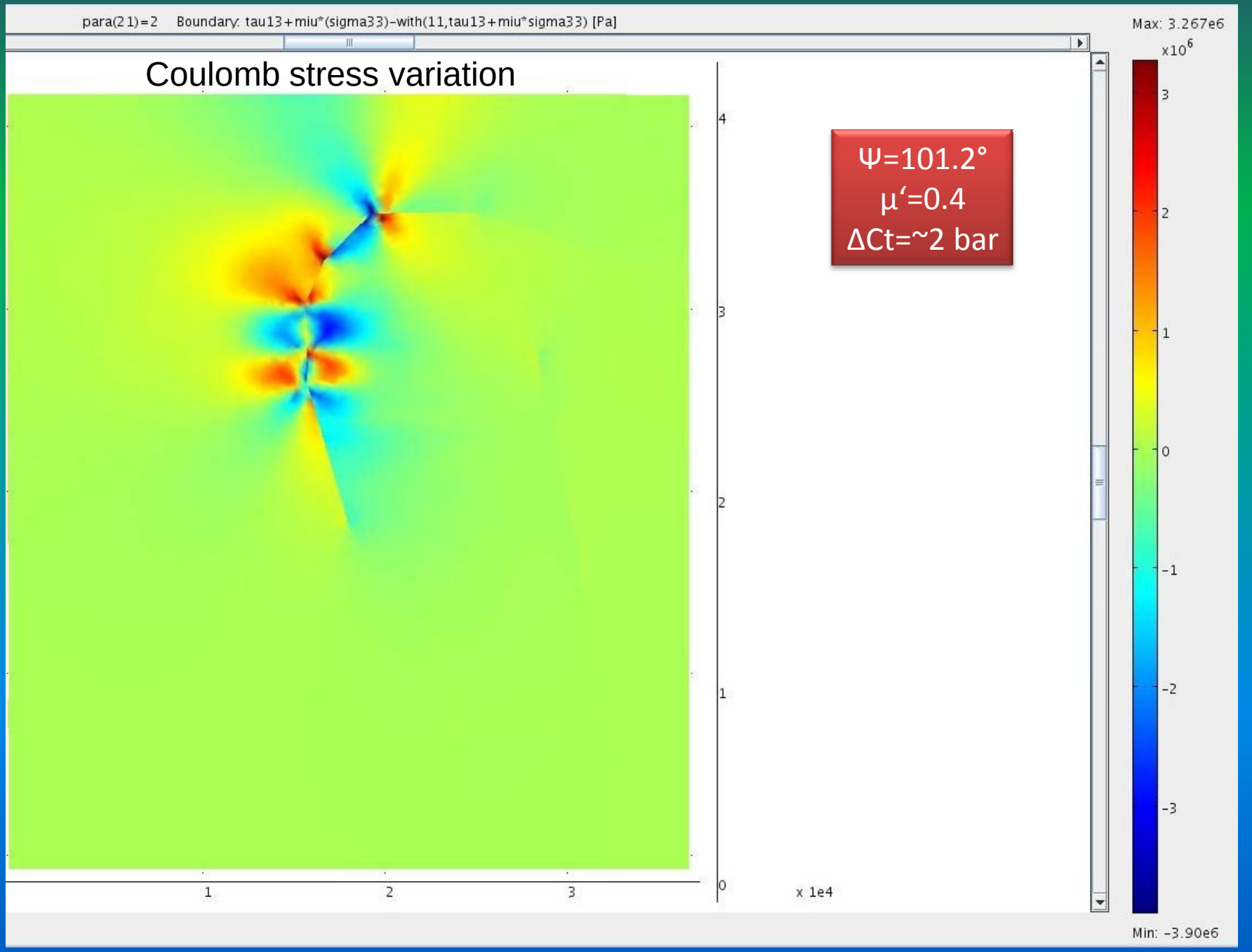
para(21)=2 Boundary: tau13+miu*(sigma33)-with(11,tau13+miu*sigma33) [Pa]
Max: 3.267e6
x10^6
3
2
1
0
-1
-2
-3
Min: -3.90e6
Coulomb stress variation
Ψ=101.2°
μ‘=0.4
ΔCt=~2 bar
4
3
2
1
0
1
2
3
x 1e4

Conclusions

The use of a model with a precise multi-layer stratification with topografy, dikes and tectonic structures shows a better “fit” with recorded data respect to analytical approach (simple tabular dislocation model [Okada, 1985] in a simple elastic half-space without heterogeneity, faulting and gravitational load conditions). For this reason the low accuracy of analytical models used for the analysis of the deformation path induced by eruptive activity is a limitation and its use is still an open problem.

By FEM model the entire deformation field caused by dike rising for 2002-2003 eruption, have been computed; in particular a deformation field in the eastern flank of Etna, in response to the dike rising, has been accurately reproduced .

Finally the importance of the tectonic control for the eastern flank strain distribution has been also demonstrated: the kinematics of Pernicana and Acitrezza faults (as known from recorded data) is in good agreement with FEM, while for Timpe fault it seems to be opposite. This is because Pernicana Fault and Acitrezza Fault are related in volcano-tectonic processes (Local stress field induced by dike rising along NE e S Rift), while movements on Timpe Fault are induced by a regional stress field (WNW-ESE extension). Trecastagni Fault has instead an optimal orientation respect to both the local field and the regional field, so the deformation pattern computed with FEM is similar to the recorded one.

End presentation

Analytical Okada model

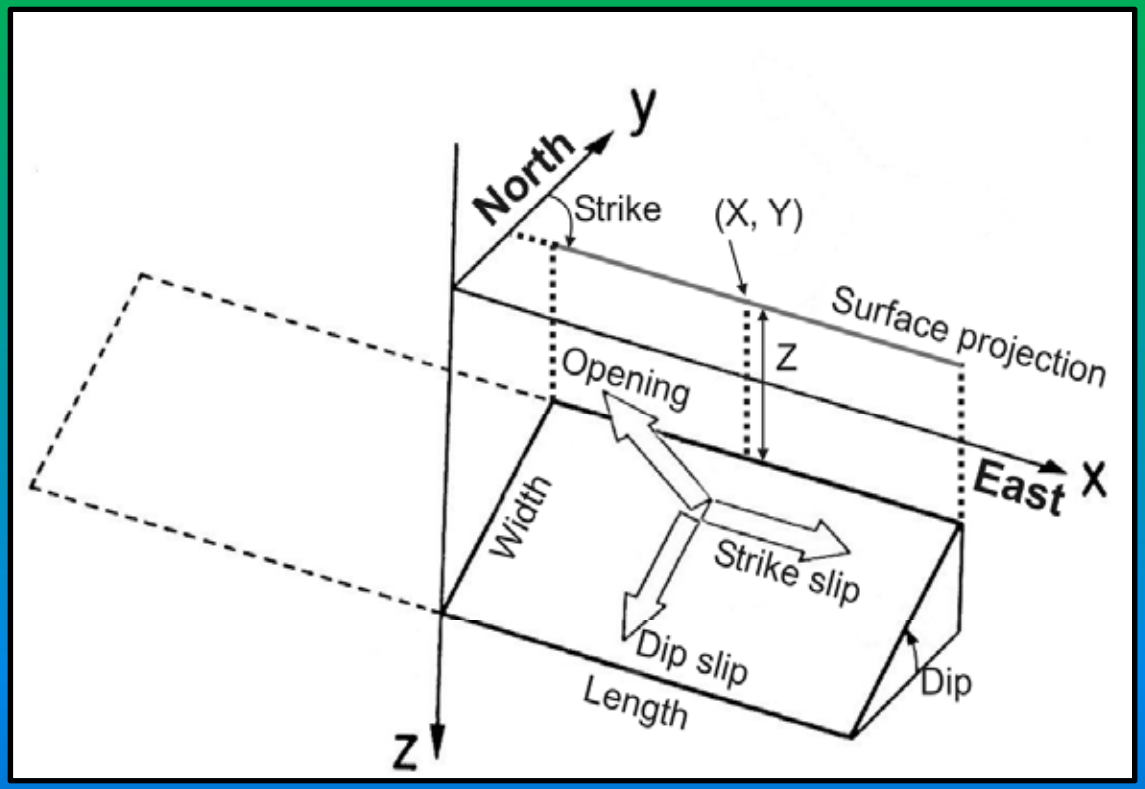

The Okada model is a tabular dislocation model described by 10 parameters: coordinates of the top centre (X, Y, Z), dimensions of the structure (length and width), orientation (strike and dip) and displacements of the dislocation (strike slip, dip slip, opening).

Technical Data

The origin of the computational domain is at:

O : (484200;4149600;0) UMT WGS 84 [in metri]

Pernicana fault west segment:

P1(503401; 4184226;0)
P2(508873; 4184305;0)

Pernicana fault east segment:

P1(503401; 4184226;0)
P2(519264; 4181235;0)